Sex Plant Reprod (1999) 11:297–322

ORIGINAL PAPER

**Paul M. Sanders · Anhthu Q. Bui · Koen Weterings
Katherine N. McIntire · Yung-Chao Hsu
Pei Yun Lee · Mai Thy Truong · Thomas P. Beals
Robert B. Goldberg**

Anther developmental defects in *Arabidopsis thaliana* male-sterile mutants

Received: 15 October 1998 / Revision accepted: 19 November 1998

Abstract We identified *Arabidopsis thaliana* sterility mutants by screening T-DNA and EMS-mutagenized lines and characterized several male-sterile mutants with defects specific for different anther processes. Approximately 44 and 855 sterile mutants were uncovered from the T-DNA and EMS screens, respectively. Several mutants were studied in detail with defects that included the establishment of anther morphology, microspore production, pollen differentiation, and anther dehiscence. Both non-dehiscencing and late-dehiscencing mutants were identified. In addition, pollenless mutants were observed with either apparent meiotic defects and/or abnormalities in cell layers surrounding the locules. Two mutant alleles were identified for the *POLLENLESS3* locus which have defects in functional microspore production that lead to the degeneration of cells within the anther locules. *pollenless3–1* contains a T-DNA insertion that co-segregates with the mutant phenotype and *pollenless3–2* has a large deletion in the *POLLENLESS3* gene. The *POLLENLESS3* gene has no known counterparts in the GenBank, but encodes a protein containing putative nuclear localization and protein-protein interaction motifs. The *POLLENLESS3* gene was shown recently to be the same as *MS5*, a previously described *Arabidopsis thaliana* male-sterility mutant. Three genes were identified in the *POLLENLESS3* genomic region: *GENEY*, *POLLENLESS3*, and *β9-TUBULIN*. The segment of the *Arabidopsis thaliana* genome containing the *POLLENLESS3* and *β9-TUBULIN* genes is duplicated and present on a different chromosome. Analysis of the *POLLENLESS3* expression pattern determined that the 1.3-kb POLLENLESS3 mRNA is localized specifically within meiotic cells in the anther locules and that POLLENLESS3 mRNA is present only during late meiosis.

Key words *Arabidopsis* · Anther development · T-DNA and EMS mutagenesis · Male-sterility mutants · Gene duplication · Meiosis

P.M. Sanders · A.Q. Bui · K. Weterings · K.N. McIntire[1]
Y.-C. Hsu · P.Y. Lee · M.T. Truong · T.P. Beals[2]
R.B. Goldberg (✉)
Department of Molecular, Cell and Developmental Biology,
University of California, Los Angeles, CA 90095–1606, USA
e-mail: bobg@ucla.edu
Tel. +1-310-825-9093; Fax +1-310-825-8201

Present addresses:
[1]Duke University School of Medicine, Durham, NC 27713, USA
[2]Cereon Genomics, One Kendall Square, Cambridge,
MA 02139, USA

Introduction

Anther development initiates with the emergence of the stamen primordia in the third whorl of the floral meristem and concludes with the release of pollen grains at dehiscence (Goldberg et al. 1993). Within the stamen primordia cell-specification and differentiation events give rise to mature anther cell types and generate the morphology of the anther and the filament. In many flowering plants, the anther has a four-lobed structure containing a stereotyped cell-type pattern that is repeated in each lobe (Goldberg et al. 1993). Microsporogenesis occurs within the reproductive locule of each lobe when the sporogenous cells enter meiosis to generate haploid microspores. Histospecification, morphogenesis, and meiotic events constitute phase one of anther development (Koltunow et al. 1990; Goldberg et al. 1993). The molecular processes that direct cell specification, differentiation, and pattern formation in the developing stamen primordia during phase one are not known. By contrast, phase two of anther development involves the functional programs that occur within differentiated anther cell types after tetrads have formed in the locules (Koltunow et al. 1990; Goldberg et al. 1993). The microspores differentiate into pollen grains, the filament elongates, the anther enlarges and expands, cell degeneration occurs, and the anther enters a dehiscence program that ends with flower opening (Goldberg et al. 1993). Dehiscence results in anther wall breakage at the stomium region located between the two locules of each anther half, or theca, and the release of pollen grains for subsequent polli-

nation and fertilization. How pollen grain differentiation, cell degeneration, and dehiscence events are coordinated during phase two of anther development is not known.

We initiated a genetic approach to identify mutants defective in anther development. Anther developmental defects can generate male-sterile phenotypes that can be identified in sterility mutant screens. Male-sterile mutants have been reported in a large number of plant species (Rick 1948; Van Der Veen and Wirtz 1968; Albertsen and Phillips 1981; Kaul 1988). These include mutants defective in anther morphology, microsporogenesis, pollen development, and pollen function. Recent interest has focused on mutagenesis screens in *Arabidopsis thaliana* for the isolation of male- and female-sterility mutants (Moffatt and Somerville 1988; Chaudhury et al. 1992, 1994 a,b; Aarts et al. 1993; Chaudhury 1993; Dawson et al. 1993; Modrusan et al. 1994; He et al. 1996; Peirson et al. 1996, 1997; Glover et al. 1996, 1998; Hulskamp et al. 1997; Taylor et al. 1998). These mutants can be distinguished from wild-type plants by the absence of silique development (Van Der Veen and Wirtz 1968). Our long-term goal is to identify mutants in *Arabidopsis thaliana* that are defective in the differentiation of anther cell types and in the anther dehiscence program.

We carried out a number of screens to identify *Arabidopsis thaliana* male-fertility mutants. Two approaches were used: (1) T-DNA insertional mutagenesis (Feldmann and Marks 1987; Feldmann 1991; Forsthoefel et al. 1992) and (2) ethyl methane sulfonate (EMS) chemical mutagenesis (Van Der Veen and Wirtz 1968; Redei and Koncz 1992). The T-DNA lines were screened to permit the isolation of T-DNA-tagged genes and their wild-type alleles with the expectation that gene function "knock-outs" would be generated by the T-DNA insertion (Feldmann 1991). By contrast, the EMS screen was initiated to attempt to saturate the *Arabidopsis thaliana* genome for male-fertility mutations (Redei and Koncz 1992). Our goal was to obtain a wide range of male-sterile phenotypes and, in particular, to identify genes involved in the anther dehiscence pathway.

Here we report the characterization of 16 recessive male-sterility mutants that belong to four general phenotypic classes. We focused on pollenless mutants to search for defects in early anther developmental processes, and on dehiscence mutants to enable us to investigate stomium region development and function. Two different dehiscence mutants were characterized. *non-dehiscence1* undergoes an abnormal cell death program during phase two of anther development and fails to dehisce at flower opening. By contrast, pollen release in the *delayed-dehiscence1* mutant occurs later than that observed in wild-type anthers and after the stigmatic papillae are no longer receptive to pollination. We identified six mutants in which the terminal anther phenotype was pollenless. Each segregated with a 3:1 F2 ratio indicating that sporophytic processes are disrupted in the mutant anthers. The six lines belong to four genetic complementation groups and have different defects leading to a pollenless phenotype. We determined that one of these lines, *pollenless3–1*, has a T-DNA insert that co-segregates with the mutant phenotype. This enabled the identification of the disrupted gene and its wild-type counterpart. A second mutant allele, *pollenless3–2*, has a 1-kb deletion in the *POLLENLESS3* gene. Both the *pollenless3–1* and *pollenless3–2* alleles fail to produce functional microspores within the anther locules as a result of an apparent defect in meiosis. The *POLLENLESS3* gene has no known counterparts in public databases, but encodes a protein with putative protein-protein interaction and nuclear localization motifs. In situ hybridization studies demonstrated that the POLLENLESS3 mRNA accumulates transiently during late meiosis in meiotic cells within the anther locule. Together, our results describe a rich collection of male-sterile mutants defective in different anther processes, and demonstrate that the *POLLENLESS3* gene is expressed specifically during meiosis and is essential for normal microspore and pollen grain production.

Materials and methods

Mutant isolation and genetic analysis

Screen 1

Five thousand T-DNA mutagenized lines of *Arabidopsis thaliana* ecotype Wassilewskija (Ws), generated by Dr. Ken Feldmann, were screened for male and female fertility mutants at the University of Arizona in November, 1991 (Feldmann and Marks 1987; Feldmann 1991; Forsthoefel et al. 1992; Modrusan et al. 1994). Fertility mutants were identified as plants which lacked siliques and excluded floral mutants and dwarf mutants which had been identified and removed prior to our screen. Fertility mutants were identified, examined for defects in pistil and stamen morphologies, and crossed with wild-type pollen. Female fertility mutants were characterized in the laboratory of Dr. Robert Fischer, University of California, Berkeley (Modrusan et al. 1994; Klucher et al. 1996). Male sterility mutants are reported in this paper and were made available to a number of other laboratories (He et al. 1996; Glover et al. 1996, 1998; Ross et al. 1997). This mutant collection can be obtained from the Ohio State University Seed Stock Center (ARBC numbers cs2361 to cs2605).

Screen 2

An additional 1600 *Arabidopsis thaliana* (Ws) T-DNA mutagenized lines, also generated by Dr. Ken Feldmann, were obtained from the Ohio State University Seed Stock Center (ARBC numbers cs6401 to cs6480) as "pools" of 20 lines. These pools were sown and screened for male fertility mutants at UCLA in November, 1995. The stamen morphology of these plants was examined and the mutants were crossed with wild-type pollen.

Screen 3

Four hundred vacuum-transformed *Arabidopsis thaliana* ecotype Columbia T-DNA mutagenized lines were obtained from the laboratory of Dr. Robert Fischer. These individual lines were examined at UCLA in October, 1997, as described in Screen 1.

Screen 4

We completed three small-scale ethyl methane sulfonate (EMS) mutagenesis screens of both individual lines (1000 lines of mutagenized *Arabidopsis thaliana* ecotype Columbia, Dr. Robert Fi-

scher) and pools (mutagenized *Arabidopsis thaliana* ecotype Columbia, Dr. Chris Somerville, Stanford University and Dr. Gary Drews, University of Utah). We also obtained male-sterile mutants from other laboratories: *delayed-dehiscence5*, a tissue culture generated T-DNA insertion mutant (Dr. Chentao Lin, UCLA); TJ421–3-3, an anther pattern mutant (Dr. Tom Jack, Dartmouth College, originally identified by Dr. Gary Drews).

Screen 5

We mutagenized 20 000 *Arabidopsis thaliana* ecotype Landsberg erecta (Ler) seeds with EMS (Redei and Koncz 1992). Seeds were imbibed overnight and then shaken in 10 mM EMS for 15 h. The M1 seeds were rinsed ten times, mixed in 0.1% agarose, and planted in 20 flats at approximately 1000 seeds per M1 flat (30.5×91.4 cm). The flats were vernalized for 3 days at 4°C prior to transfer to the greenhouse. We estimated that approximately 58% of the M1 seedlings germinated and survived the EMS treatment. M2 seeds were collected as 20 pools from approximately 600 M1 plants in each flat and then dried for 5–7 days. The M2 seeds were placed in 0.1% agarose and chilled for 3 days at 4°C prior to planting in the greenhouse. We planted approximately 12 000 seeds from each M2 pool and a primary screen of the 180 000 surviving M2 plants was carried out at UCLA in May, 1998. Using a Poisson distribution we estimated that this number of M2 plants is sufficient to have a 70% probability of finding each fertility mutation generated by EMS within the population of 12 000 M1 plants [N/M1 plant=ln (1–0.7)/ln (1–0.125) (Dr. Ken Feldmann, personal communication; Redei and Koncz 1992)]. Our goal was to determine the range of male-sterile mutants that could be identified and, in particular, the range of phenotypes obtained within the dehiscence class. Only mutants with either a dehiscence or anther pattern phenotype were crossed with wild-type pollen to generate lines for future study.

Male-sterile mutants from screens 1–4 were confirmed by following the inheritance of the mutant phenotype in lines established by crosses with wild-type pollen. These lines were maintained as heterozygotes (MS/ms) and their progeny segregated for wild-type and male-sterile plants. Mutants were characterized by examination of flowers and anthers using a dissecting microscope (Olympus Model SZH, Olympus, Lake Success, N.Y.). Complementation crosses were carried out with pollen from the heterozygous (MS/ms) plants applied to male-sterile plants (ms/ms) for mutants from the pollenless and dehiscence classes. If the two lines represented mutations at different gene loci, then 100% wild-type progeny were expected. If the two lines represented mutant alleles of the same locus, then the progeny were expected to segregate 50% wild-type to 50% male-sterile plants.

Light microscopy

Bright-field photographs of individual flowers were taken using a dissecting microscope (Olympus Model SZH). Mutant and wild-type flowers were fixed overnight in FAA (50% ethanol, 5.0% glacial acetic acid, 3.7% formaldehyde), dehydrated in a graded ethanol series (2×50%, 60%, 70%, 85%, 95%, 3×100%), embedded in Spurr's epoxy resin (Spurr 1969; TedPella, Redding, Calif.) or LR-White resin (Polysciences, Warrington, Pa.), and sectioned (1 μm) using a microtome (LKB Ultratome V, LKB, Bromma, Sweden). Anther transverse sections were stained in 1% toluidine blue at 42°C for 1–2 h for Spurr's resin sections, or for 5–10 min for LR-White plastic sections. Bright-field photographs of the anther cross-sections were taken using a compound microscope (Olympus Model BH2). All photographs were taken with Kodak Gold 100 film (ISO 100/21).

Scanning electron microscopy

Wild-type and mutant inflorescences were fixed overnight in FAA, dehydrated in a graded ethanol series as described above, and critical point dried in liquid CO_2. Individual anthers and pollen from flowers that corresponded to a specific stage of wild-type anther development were mounted on scanning electron microscope stubs. Pollen grains from dehiscence mutants were obtained by manually opening the anthers after critical point drying of the sample. Mounted samples were coated with palladium-gold in a sputter coater (Hummer, Alexandria, Va.) and then examined in an autoscan scanning electron microscope (ETEC, Hayward, Calif.) with an acceleration voltage of 10 kV. Photographs were taken using Polaroid type 55 film.

Genomic DNA isolation and T-DNA insert analysis

Arabidopsis thaliana ecotype Ws genomic DNA was isolated from *pollenless3–1*, *pollenless3–2*, and wild-type plants (Murray and Thompson 1980). The DNA (1–2 μg) was digested with restriction endonucleases (Life Technologies, Gibco-BRL, Gaithersburg, Md.), separated in 0.6–0.8% agarose gels (1× TAE buffer), and transferred to Nytran membranes (Schleicher and Schuell, Keene, N.H.).

The DNA blots were hybridized with T-DNA right and left border sequences labeled with ^{32}P-dCTP by random primer synthesis (Feinberg and Vogelstein 1983). The T-DNA right border probe was a HindIII fragment from pKC7H23 (Dr. P. Zambryski, University of California, Berkeley; Zambryski et al. 1980) containing 2.3 kb of the T-DNA right border. The T-DNA left border probe was a HindIII fragment from pBSH10 (Dr. P. Zambryski, University of California, Berkeley; Zambryski et al. 1980) containing 2.9 kb of the T-DNA left border.

Plasmid rescue experiments

Plasmid rescue experiments to isolate plant flanking sequence clones were performed according to Behringer and Medford (1992), except that the genomic DNA ligation step was performed in a 500-μl volume. Rescued T-DNA border-plant junction clones were confirmed by restriction endonuclease mapping and hybridization to genomic DNA from wild-type and male-sterile plants.

Isolation of *Arabidopsis* wild-type genomic clones

Plant sequences flanking both sides of the T-DNA insert in *pollenless3–1*, identified by plasmid-rescue, were utilized to screen an *Arabidopsis thaliana* ecotype Ws wild-type genomic library (a gift from Dr. Ken Feldmann). Three successive rounds of screening were performed to isolate individual lambda clones. DNA labelling, library screening, and lambda DNA isolation were carried out as described by Jofuku and Goldberg (1988).

Poly(A) mRNA isolation, RNA blots, and Marathon cDNA amplification

Polysomal RNA was isolated from (1) a developmental pool of unopened floral buds, (2) a mixture of leaves and stems, (3) roots, and (4) siliques from wild-type *Arabidopsis thaliana* ecotype Ws plants (Cox and Goldberg 1988). Poly(A) mRNA was isolated using either oligo(dT) cellulose or PolyATract magnetic beads (Promega, Madison, Wis.). The poly(A) mRNA was size-fractionated by electrophoresis in formaldehyde gels and blotted to Nytran membranes (Schleicher and Schuell) as outlined in Koltunow et al. (1990). The floral bud poly(A) mRNA was also used for Marathon cDNA amplification (Clontech, Palo Alto, Calif.).

Reverse transcription-polymerase chain reaction

First-strand cDNAs were synthesized from 0.5 μg of polysomal poly(A) mRNA isolated from inflorescences (pooled stages), leaves and stems, and roots of *Arabidopsis thaliana* ecotype Ws. Reverse transcription (RT) was carried out using Superscript II

Moloney Murine leukemia virus reverse transcriptase (Life Technologies, Gibco-BRL) according to the supplier's protocol accompanied with the Superscript II. One-fifth of the RT reaction was amplified by the polymerase chain reaction (PCR) in a 50 µl volume using sequence-specific primers and *Taq* DNA polymerase (Life Technologies, Gibco-BRL) and the GeneAmp PCR system 9700 (Perkin-Elmer, Branchburg, N.J.). The PCR profile was: 96°C for 3 min, followed by 30 cycles of 96°C for 0.5 min; 65°C for 1 min; 72°C for 1.5 min; and 72°C for 7 min. The following primers were used: *POLLENLESS3*: 5′-agaggaggagaccaccgtattcttg-3′ and 5′-ggttcatctccgcattcactctct-3′; *POLLENLESS3-LIKE1*: 5′-aagtctgggaggattacagaggtcg-3′ and 5′-cgtcattagtagtcgaggctgctgt-3′. One-fifth of the PCR reaction volume was fractionated on a 0.8% agarose gel containing ethidium bromide.

Isolation of 5′ and 3′ RACE cDNA clones

Gene-specific primers were designed to identify 5′ and 3′ rapid amplification of cDNA ends (RACE) cDNA products generated from a wild-type *Arabidopsis thaliana* ecotype Ws inflorescence Marathon cDNA. Gene-specific primers were designed from identified open reading frames and matched to the Marathon cDNA amplification protocol specifications (*GENEY*: 5′RACE primer 5′-ggttcctgaactttggaagctgtggct-3′; 3′RACE primer 5′-ggagtcagatcctttcttggccatttcc-3′; *POLLENLESS3*: 5′RACE primer 5′-tagctttcgagcagcacctctcgtctc-3′). The cDNA RACE products were reamplified, gel purified (GeneClean, Bio101, Vista, Calif.), and cloned into the pCR2.1 vector (TA Cloning, Invitrogen, Carlsbad, Calif.).

DNA and protein sequence analysis

DNA was sequenced either manually by using the Sequenase Kit (United States Biochemical, Cleveland, Ohio) or by using the UCLA Life Sciences Automated ABI Sequencing Facility. Sequencing was initiated by use of either commercial primers or gene-specific primers designed from a previous sequencing result. All protocols for the sequencing of PCR products and plasmid templates were as described by ABI (Perkin-Elmer/Roche Molecular, Branchburg, N.J.).

Compilation and analysis of DNA sequence data were carried out by using the Genetics Computer Group (GCG) Wisconsin programs. ORFs and exon-intron junctions were identified by using NetPlantGene (Hebsgaard et al. 1996, http://genome.cbs.dtu.dk/services/NetPGene/). DNA sequence comparisons were performed using the NCBI GenBank BLAST programs (Altschul et al. 1990, 1997, http://www.ncbi.nlm.nih.gov/). DNA alignments were carried out in the DNA Inspector program. (Textco, West Lebanon, N.M.). ProfileScan (http://www.isrec.isb-sib.ch/software/PFSCAN_form.html) and PSORT (Nakai and Kanehisa 1992, http://cookie.imcb.osaka-u.ac.jp/nakai/psort.html) were used to identify protein motifs. PAIRCOIL (Berger et al. 1995, http://theory.lcs.mit.edu/~bab/paircoil.html) was used to search for coiled-coil regions within protein sequences. Protein secondary structure predictions were undertaken through nnPredict (Kneller et al. 1990, http://www.cmpharm.ucsf.edu/~nomi/nnpredict.html). Primers were designed by use of Primer3 (http;//www-genome.wi.mit.edu/cgi-bin/primer/primer3.cgi) and the GCG Wisconsin programs. The *POLLENLESS3-LIKE1* gene region sequence within chromosome 5 was obtained from KAOS (Kaneko et al. 1998; http://www.kazusa.or.jp/arabi/). Protein tertiary structure analysis based upon amino acid sequence was undertaken through 123D Threading (Alexandrov et al. 1995, http://www-lmmb.ncifcrf.gov/~nicka/123D.html) and the UCLA-DOE Fold Recognition server (Fischer and Eisenberg 1996, http://fold.doe.mbi.ucla.edu).

Isolation of a genomic clone containing the *pollenless3–2* gene

Sequencing primers known to flank the *pollenless3–2* deletion were used to isolate genomic DNA fragments from both wild-type and *pollenless3–2* plants by PCR amplification. The two primers were 5′-cg[gaattc]aaggaatggacgagatgg-3′ and 5′-cg[ggatcc]gattctccttacgtcagagcc-3′. The brackets refer to EcoRI and BamHI restriction endonuclease sites that were added to the primers to facilitate cloning of the PCR products. The PCR amplification products were gel purified (GeneClean, Bio101) and cloned into the pCR2.1 vector (TA Cloning, Invitrogen).

In situ hybridization studies

Arabidopsis thaliana ecotype Ws inflorescences from wild-type and *pollenless3–2* plants were fixed, processed, and sectioned as

Table 1 Fertility mutants identified in *Arabidopsis* mutant screens

Class	Mutant phenotypes	Screen			
	Description	5000 T-DNA[a]	1600 T-DNA[b]	400 T-DNA[c]	Other screens[d]
Early defect	Undeveloped anther	–	–	–	1
Pollenless	Anthers devoid of pollen grains	5	2	–	–
Defective pollen	Abnormal pollen in dehisced anthers[e]	3	2	2	–
Pollen function/ Female sterile	Visually wild-type pollen grains[e]	12	–	–	–
Stamen length	Reduced filament extension	–	–	3	–
Dehiscence	Anthers defective in pollen release	3	–	1	3
Pattern	Alteration in anther morphology and/or locule number	–	–	1	1
Floral	Altered floral organ development	–	3	2	–
Reduced fertility	Consistently short siliques	4	–	1	–

[a] Screened as individual families. Identified lines segregating a mutant phenotype (see Materials and methods, Screen 1). Primary screen selection for mutants defective in anther development. Floral and dwarf mutants were identified previously. Sterile mutants that appeared to contain wild-type pollen grains were not included in the secondary screen. Female sterile lines from this screen were studied in the lab of Dr. Robert Fischer, UC Berkeley (*bel* – Modrusan et al. 1994; Reiser et al. 1995; *ant* – Klucher et al. 1996)

[b] Screened as pools of twenty lines each. Identified individual mutant plants (see Materials and methods, Screen 2)

[c] Screened as individual families (see Materials and methods, Screen 3)

[d] These mutants came from our initial small-scale EMS mutagenesis screens, or from male-sterile lines given to us from other laboratories (see Materials and methods, Screen 4)

[e] Mutants in the defective pollen class had visibly abnormal pollen grains at dehiscence. These pollen grains had a dark color and/or a sticky appearance in the dissecting microscope (see Materials and methods). By contrast, mutants in the pollen function/female sterile class had pollen grains that were indistinguishable from those of wild-type plants in the dissecting microscope

Table 2 *Arabidopsis* fertility mutants identified in a large-scale EMS screen[a]

Class[b]	Mutant phenotype description		Number
Early defect	Undeveloped anther (*fil-like*[c])		2
Pollenless	Anthers devoid of pollen grains		101
Defective pollen/female sterile	Abnormal and/or reduced pollen in dehisced anthers[d]		76
Pollen function/female sterile	Visually wild-type pollen grains [d]		129
Stamen length	Reduced filament extension		15
Dehiscence	Anthers defective in dehiscence		273
	non-dehiscent anthers with pollen	4	
	non-dehiscent anthers without pollen	69	
	late-dehiscent anthers with pollen	145	
	late-dehiscent anthers without pollen	55	
Pattern	Alteration in locule number		56
	ant-like [c, e]	14	
	ettin-like [c, f]	14	
	not *ettin-like* or *ant-like* [g]	14	
	Alteration in anther morphology[g]	14	
Floral	Altered floral organ development		150
	non-homeotic [h]	81	
	unusual pistils [i]	23	
	homeotic	46	
	agamous-like [c]	1	
	ap2-like [c]	24	
	ap3/pi-like [c]	18	
	leafy-like [c]	1	
	other [j]	2	
Reduced fertility [k]	Consistently short siliques		53
cer[l]			30

[a] 180 000 M2 plants were screened for fertility mutants from 20 M1 pools of 600 lines each. In all 855 fertility-related mutants were identified. Only mutants identified in the dehiscence and pattern classes were crossed with wild-type plants to obtain F1 seeds (see Materials and methods, Screen 5)

[b] The primary goal of the EMS screen was to identify mutants defective in the anther dehiscence process. Each mutant that affected dehiscence was included in the dehiscence class, even though other traits might have been affected (e.g., pollenless). As such, the mutants in other classes may have been underestimated

[c] A number of mutants in this screen were identified visually as similar to known mutants. We described these mutants as "*-like*" (e.g., *fil-like*), but did not confirm the visual identification by crossing or mapping

[d] Defective pollen mutants had visibly abnormal pollen grains at dehiscence (n=30) and/or a reduced level of pollen grains (n=46). Pollen function/female sterile mutants had pollen grains that were indistinguishable in the dissecting microscope

[e] The floral phenotype of these mutants was similar to *aintegumenta1* (*ant1*) (Klucher et al. 1996). Anthers had two lobes with a single locule each, and the plants appeared to be female sterile

[f] The floral phenotype of these mutants was similar to *ettin* (Sessions and Zambryski 1995; Sessions et al. 1997). Anthers had a variable number of locules, ranging from one to four, and the plants appeared to be female sterile

[g] The anthers of these mutants had alterations in size, shape, and lobe number, but did not appear to be either *ant-like* or *ettin-like*

[h] Altered floral organ development where the phenotypes do not appear to be similar to homeotic floral mutations described previously (Coen and Meyerowitz 1991)

[i] Visible defect in pistil structure (e.g., unfused carpel, abnormal stigma). Other floral organs appear normal

[j] Altered floral organ identity which does not correspond with a described homeotic phenotype

[k] Not all of the reduced-fertility-phenotype mutants were cataloged in this screen. Therefore, the number listed in this table is an underestimate

[l] *eceriferum* (*cer*) mutants affect epicuticular wax biosynthesis, and some *cer* mutants affect pollen fertility (McNevin et al. 1993). One of these mutants was also classed as *fil-like*

described previously (Cox and Goldberg 1988; Yadegari et al. 1994; Beals and Goldberg 1997). The synthesis of single-stranded-labeled RNA probes, in situ hybridization, slide washing, and exposure to Kodak NTB-2 emulsion was carried out as described by Yadegari et al. (1994) and Beals and Goldberg (1997). RNAs were labeled with ^{33}P-UTP (Beals and Goldberg 1997). The in situ hybridization experiment was carried out using both sense and anti-sense probes generated from *POLLENLESS3* 5′RACE cDNA clones. Sense and antisense ^{33}P-rRNA probes were used as controls (Delsney et al. 1983). Bright-field and dark-field photographs were taken using an Olympus compound microscope (Olympus Model BH2) with Kodak Gold 100 ASA film (ISO 100/21).

Results

Male-sterile mutants were identified in T-DNA and EMS mutagenesis screens

We screened 7000 T-DNA mutagenized *Arabidopsis thaliana* lines (Table 1) and 180 000 EMS treated lines (Table 2) to identify mutants defective in anther development and/or function (see Materials and methods). Our primary screens identified mutagenized lines that segregated sterile plants by the absence of silique development after flower opening (Van Der Veen and Wirtz 1968). We visually examined the flowers and floral organs of each sterile line at different developmental periods and identified nine general classes of fertility mutants: (1) early anther defect, (2) pollenless, (3) defective pollen, (4) pollen function/female sterile, (5) stamen length, (6) non- or late-dehiscence, (7) anther pattern, (8) floral, and (9) reduced fertility. A description of the typical phenotype for each of these mutant classes is listed in Table 1.

Figure 1 compares recently opened flowers from representative mutant classes with those of wild-type plants. In wild-type, the filament of each stamen elongated to position the anther at the height of the stigma (Fig. 1A). The anthers have just dehisced and released pollen grains (Fig. 1A). Each mutant class, by contrast, exhibited a specific floral or stamen defect. For example, *undeveloped anther*, representative of the early defect class, had stamens with filament-like structures that did not contain anthers (Fig. 1E). The *undeveloped anther* mutant has been described previously, has defects in other floral organs, and is allelic to *fil*, a pleiotrophic flower mutant (Komaki et al. 1988; Chaudhury et al. 1992; Goldberg et al. 1993; Okada and Shimura 1994). Anthers of *pollenless3–2*, a member of the pollenless class, were often flattened in appearance just prior to dehiscence and were devoid of pollen grains (Fig. 1B). By contrast, abnormal-looking pollen grains were released at dehiscence from *defective-pollen3* anthers, a member of the defective-pollen class (Fig. 1C). The anthers of a similar class, designated as pollen function/female sterile, also released pollen grains at dehiscence but these pollen grains were visibly indistinguishable from those of wild type (Table 1; data not shown). Mutants in the pollen function/female-sterile class were probably due to defects in either post-pollination pollen functions (i.e., germination, tube growth; Hulskamp et al. 1995), or to defects in female fertility (Modrusan et al. 1994). A fourth class, represented by *delayed-dehiscence1*, had anthers that did not dehisce at flower opening, and the undehisced anthers were indistinguishable at the light microscopy level from wild-type anthers prior to dehiscence (Fig. 1D). Finally, *fused sepals*, representative of the floral class, had sepals that were fused along their margins which impaired pollen delivery to the stigma and caused reduced fertility (Fig. 1F). Although we identified floral homeotic mutants in both the T-DNA and EMS screens, these mutants were not studied and are included in Table 2 only as an internal measure of the degree of "saturation" obtained by our EMS treatment. The floral class listed in Table 1 includes only non-homeotic mutants affecting flower development. These mutants and those in classes affecting pollen function/female sterility, stamen length, and reduced fertility were not studied further.

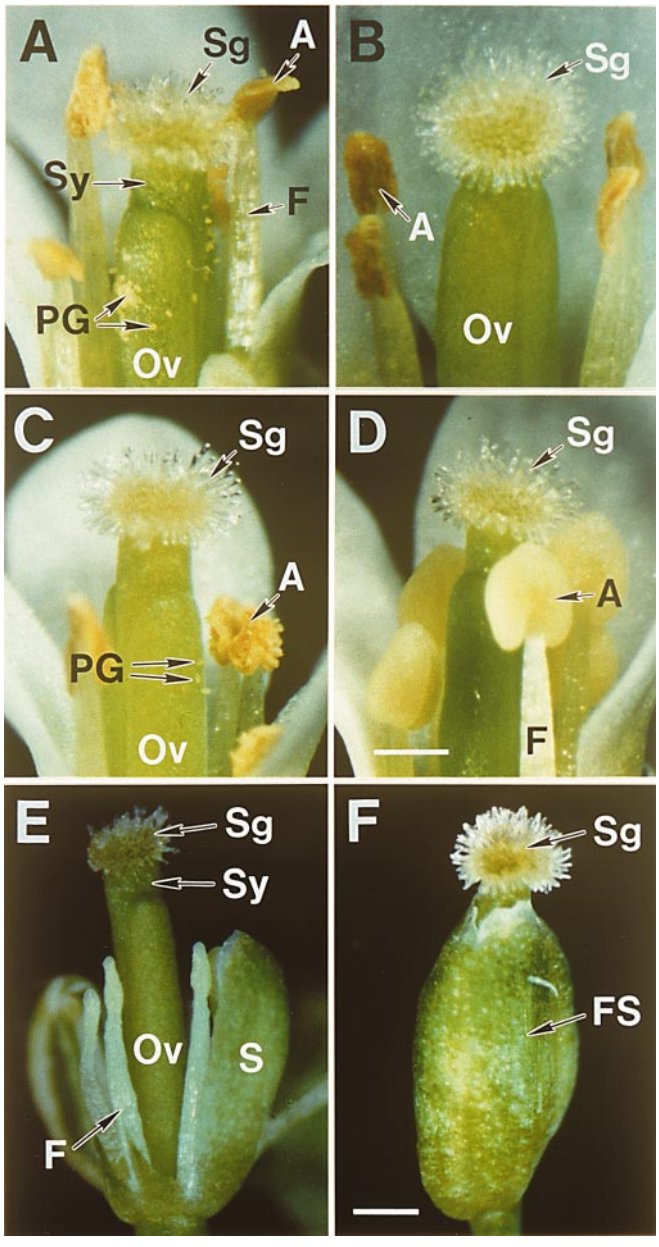

Fig. 1A–F *Arabidopsis thaliana* wild-type and mutant flowers. Open flowers were photographed by bright-field microscopy. **A** Wild type. **B** *pollenless3–2*. Identified in Screen 1 (5000 T-DNA; Table 1). **C** *defective-pollen3*. Identified in Screen 1 (5000 T-DNA; Table 1). **D** *delayed-dehiscence1*. Identified in Screen 1 (5000 T-DNA; Table 1). **E** *undeveloped anther*. Identified in Screen 4 (other screens, EMS mutagenesis; Table 1). **F** *fused sepals*. Identified in Screen 2 (1600 T-DNA; Table 1). The T-DNA in this line does not segregate with the fused sepal phenotype (data not shown). *A*, Anther; *F*, filament; *FS*, fused sepals; *Ov*, ovary; *PG*, pollen grain; *S*, sepal; *Sg*, stigma; *Sy*, style. *Bar* in **D**=250 μm and this is the scale for **A**, **B** and **C**. *Bar* in **F**=25 μm and is the scale for **E**

Table 3 Male-sterile mutants characterized from *Arabidopsis* mutant screens[a]

Mutant class	Complementation groups	Description of mutant phenotype
Early defect	*undeveloped anther*[b]	Affects floral development. Stamen does not usually develop into an anther, but has filament-like structure. Rare stamens generate pollen
Pollenless	I *pollenless1-1, 1-2* II *pollenless2* III *pollenless3-1* [c, d], *3-2*	Anther locules devoid of pollen grains. Cells derived from microspore mother cells degenerate. Tetrads and microspores are either abnormal or not present. Premature degeneration of the tapetum also occurs in *pollenless1-1* and *pollenless2*
	fat tapetum [e]	Pollenless phenotype. Mutant phenotype diverges from wild type prior to meiosis. The middle layer and tapetum enlarge and the locules collapse
Defective pollen [e]	*defective-pollen1, 2, 3* [d, f]	Aberrant pollen visualized on dehisced anthers. Meiosis and pollen development occur
Dehiscence	I *delayed-dehiscence1* [d] II *delayed-dehiscence2* III *delayed-dehiscence3* IV *delayed-dehiscence4* *delayed-dehiscence5* [e]	Anther dehiscence and pollen release are delayed preventing successful pollination
	V *non-dehiscence1*	Anthers contain pollen but do not dehisce

[a] *undeveloped anther*, *delayed-dehiscence3*, and *delayed-dehiscence4* were identified from EMS screens. *delayed-dehiscence5* was identified from a screen of tissue culture T-DNA transformation lines (Dr. Chentao Lin, UCLA). All other mutants were obtained from Feldmann T-DNA lines (see Materials and methods. Feldmann 1991; Forsthoefel et al. 1992). The Feldmann line numbers corresponding to these mutants were: *pollenless1–1*=1728, *pollenless1–2*=1180, *pollenless2*=2824, *pollenless3–1*=178, *pollenless3–2*=1097, *defective-pollen1*=783, *defective-pollen2*=1569, *defective-pollen3*=2522, *delayed-dehiscence1*=1926, *delayed-dehiscence2*=2379, *non-dehiscence1*=547, and *fat tapetum*=pool 6410 of the Feldmann T-DNA line numbers listed in the Arabidopsis Information Management System (AIMS), Arabidopsis Biological Resource Center (ABRC) seed catalog (http://aims.cps.msu.edu/aims/)

[b] Complementation crosses showed that *undeveloped anther* (Goldberg et al. 1993), previously called *antherless* (Chaudhury et al. 1992), was allelic to *fil* (Komaki et al. 1988; Okada and Shimura 1994)

[c] *pollenless3–1* was described recently as *ms5* by Glover et al. (1998) and *tdm1* by Ross et al. (1997)

[d] These three lines contain a T-DNA insert that co-segregates with the mutant phenotype

[e] Completion crosses were not carried out for these mutants

[f] *defective-pollen3* was described previously as *mei1* by He et al. (1996) and *mcd1* by Ross et al. (1997)

We obtained approximately 44 fertility mutants from our T-DNA screens (Table 1). All of these mutants were confirmed in subsequent generations from segregating F2 populations. By contrast, we obtained 855 EMS-induced fertility mutants, or approximately 7% of the 12000 M1 lines screened (Table 2). Of these, 208 mutants affected floral morphology, anther development, and/or anther formation, while 579 affected pollen function, development, or release (Table 2). An additional 68 mutants had either reduced fertility or short filament length (Table 2). The EMS screen was designed to "saturate" the *Arabidopsis thaliana* genome with fertility mutations, and, in particular, identify a large collection of mutants defective in the dehiscence pathway. We obtained 273 mutants with defects in the dehiscence process (Table 2). We also obtained a large number of mutants (46) that resembled several well-characterized floral homeotic gene loci in this screen (e.g., *ap3-like*, *ap2-like*), suggesting that we achieved "saturation," at least for some genomic regions (Table 2).

In the study reported here, we focused on male-sterile mutants that affected anther morphology, pollen formation, and dehiscence, and in which all other floral organs appeared wild-type. These mutants and their phenotypes are listed in Table 3. In each case, the male-sterile mutants were female fertile and segregated 3:1 in the F2 generation, indicating that they were the result of recessive sporophytic mutations (data not shown). Complementation crosses were carried out to determine the number of independent genetic loci identified by the male-sterile mutants of the pollenless and dehiscence classes. At least three complementation groups were identified for the five pollenless mutants, and the dehiscence mutants were represented by at least five independent genetic loci (Table 3). Three of these mutants were shown to contain a T-DNA that co-segregated with the mutant phenotype: *pollenless3–1*, *defective-pollen3*, and *delayed-dehiscence1* (data not shown; Glover et al. 1996; He et al. 1996). Preliminary studies suggested that a fourth mutant, *delayed-dehiscence5*, also had a T-DNA that co-segregated with the defective dehiscence phenotype (data not shown).

Characterization of anther and pollen morphology from representative male-sterile mutants in the scanning electron microscope

We characterized the stamens of several male-sterile mutants by scanning electron microscopy (SEM) to identify defects in anther morphology (see Materials and methods). The four-lobed structure of a wild-type *Arabidopsis thaliana* anther is shown in Fig. 2A, whereas Fig. 2B shows a wild-type anther that split open along the stom-

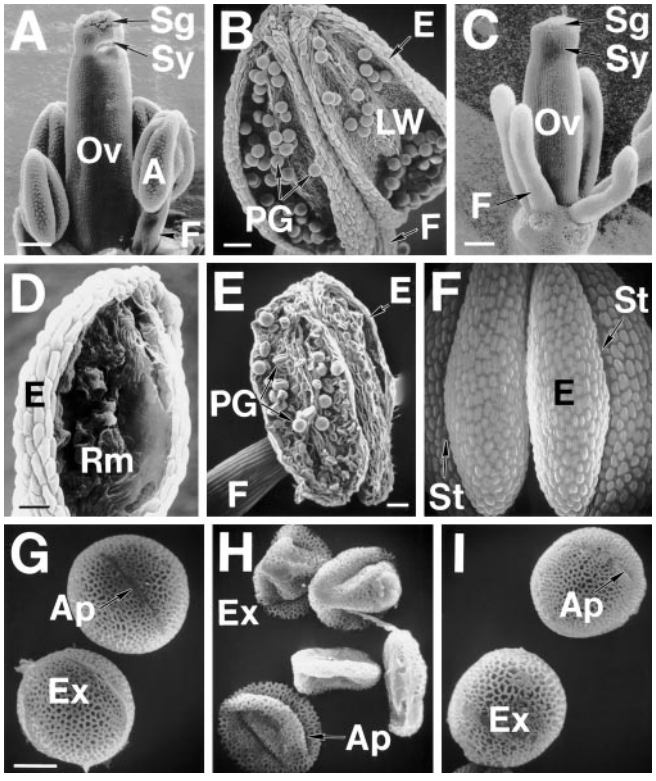

Fig. 2A–I Scanning electron micrographs of *Arabidopsis thaliana* wild-type and mutant anthers and pollen. Anthers and pollen were isolated from flowers at anthesis and were photographed in the scanning electron microscope as outlined in Materials and methods. **A** and **B** Wild-type *Arabidopsis thaliana* floral organs. Flower at stage 5 of anther development with sepals and petals removed (**A**) and dehisced anther at stage 13 (**B**). **C** *undeveloped anther* flower with sepals and petals removed. Developmental stage similar to that in (**A**). **D–F** Male-sterile anthers at stage 13. *pollenless3-2* (**D**), *defective-pollen3* (**E**), and *delayed-dehiscence1* (**F**). **G–I** Pollen grains from anthers shown in (**B**), (**E**) and (**F**), respectively. Wild-type pollen grains (**G**), *defective-pollen3* (**H**), and *delayed-dehiscence1* (**I**). *A*, Anther; *Ap*, aperture; *E*, epidermis; *Ex*, exine; *F*, filament; *LW*, inner locule wall; *Ov*, ovary; *PG*, pollen grain; *Rm*, remnants of locule contents; *Sg*, stigma; *St*, stomium; *Sy*, style. *Bar* in (**A**)=100 μm, *Bar* in (**B**)=30 μm, *Bar* in (**C**)=75 μm, *Bar* in (**D**)=20 μm, *Bar* in (**E**)=25 μm and represents the same scale for (**F**), *Bar* in (**G**)=5 μm and represents the same scale for (**H**) and (**I**)

ium and released pollen grains at dehiscence. By contrast, stamens of the *undeveloped anther* mutant did not develop anthers, but consisted of filament-like structures which terminated in a small "swelling" at their tips (Fig. 2C). The anthers of most male-sterile mutants within the pollenless, defective-pollen, and dehiscence classes were indistinguishable from those of wild type with respect to size and morphology when examined by SEM in recently opened flowers (Fig. 2D–F). However, anthers of *pollenless3–2* were devoid of pollen grains at dehiscence and often contained "remnants" of degenerated cellular material in the locule chamber (Fig. 2D). Anthers of *defective-pollen3* dehisced and contained pollen-grain-like material (Fig. 2E). The anthers of *delayed-dehiscence1* had well-developed stomium "notch" regions between each pair of lobes, but remained closed at flower opening (Fig. 2F).

We examined the pollen grains present within *defective-pollen3* and *delayed-dehiscence1* anthers using SEM, and compared these pollen grains with those of wild-type anthers. Wild-type pollen grains were spherical, had sculptured exine walls, and visible apertures were present through which the future pollen tubes could emerge (Fig. 2G). By contrast, pollen grains of *defective-pollen3* had normal-appearing exine wall sculpturing, but exhibited a collapsed morphology (Fig. 2H). The extent of this defect varied between lines of this class (data not shown). When *delayed-dehiscence1* anthers were manually opened and examined using SEM, their pollen grains were indistinguishable from those of wild–type anthers with respect to morphology and exine wall sculpturing (Fig. 2I). *delayed-dehiscence1* pollen grains were viable and capable of successful pollination (data not shown).

Arabidopsis thaliana anther development involves both cell differentation and degeneration processes

We prepared transverse sections of wild-type *Arabidopsis thaliana* anthers in order to describe the changes that occurred at the cellular level from the emergence of the stamen primordia to anther dehiscence and senescence. These sections served as a control to uncover events responsible for the loss of fertility in the male-sterile lines we investigated. We divided *Arabidopsis thaliana* anther development into 14 stages at which distinctive cellular events could be visualized at the level of the light microscope. Stages 1 to 8 represented phase one of anther development (Fig. 3), while stages 9 to 14 represented phase two of anther development (Fig. 4). Table 4 lists a summary of the key events that occurred at each stage, the cells and tissues that were present, and a cross-reference between our anther stages and those described previously for *Arabidopsis thaliana* flower and pollen development (Regan and Moffatt 1990; Smyth et al. 1990; Bowman et al. 1991).

During stages 1 to 4, cell division events occurred within the developing anther primordia to establish a bilateral structure with locule, wall, connective, and vascular regions characteristic of the mature anther (Fig. 3). Archesporial cells within the four corners of the anther primordia divided periclinally to give rise to distinct 1° parietal and 1° sporogenous cell lineages that differentiated into the endothecium, middle layer, tapetum, and microspore mother cells of the locules (Fig. 3, stage 5). Microspore mother cells underwent meiosis between stages 5 and 7 within each of the four locules and generated tetrads of haploid microspores (Fig. 3, stage 7). Microspores were released from the tetrads at stage 8 (Fig. 3) and differentiated into three-celled pollen grains (data not shown) between stages 9 and 12 (Fig. 4). Coordinated with pollen development was a general increase in anther size, degeneration of several cell layers, and

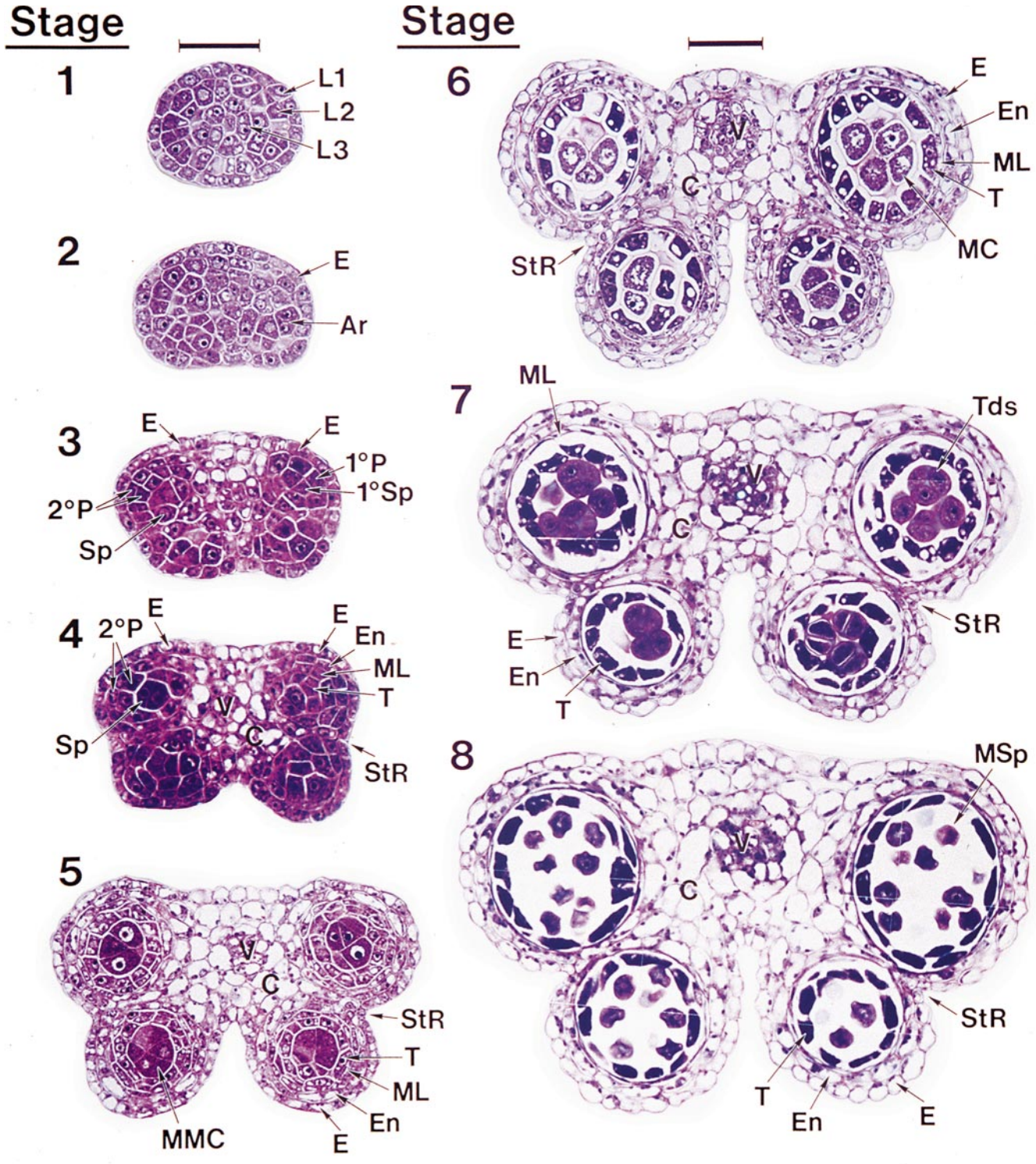

Fig. 3 Phase one of wild-type *Arabidopsis thaliana* anther development. Flowers were fixed and embedded in LR-White plastic resin and sliced into 1 μm transverse sections as described in Materials and methods. The flower sections were stained with toluidine blue and anthers were photographed by bright-field microscopy. *Ar*, archesporial cell; *C*, connective; *E*, epidermis; *En*, endothecium; *L1*, *L2*, and *L3*, the three cell-layers in stamen primordia; *MC*, meiotic cell; *ML*, middle layer; *MMC*, microspore mother cells; *MSp*, microspores; *1°P*, primary parietal layer; *2°P*, secondary parietal cell layers; *1°Sp*, primary sporogenous layer; *Sp*, sporogenous cells; *StR*, stomium region; *T*, tapetum; *Tds*, tetrads; *V*, vascular region. *Bar* over stage 1=25 μm and this is the scale for stages 1 to 4. *Bar* over stage 6=25 μm and this is the scale for stages 5 to 8

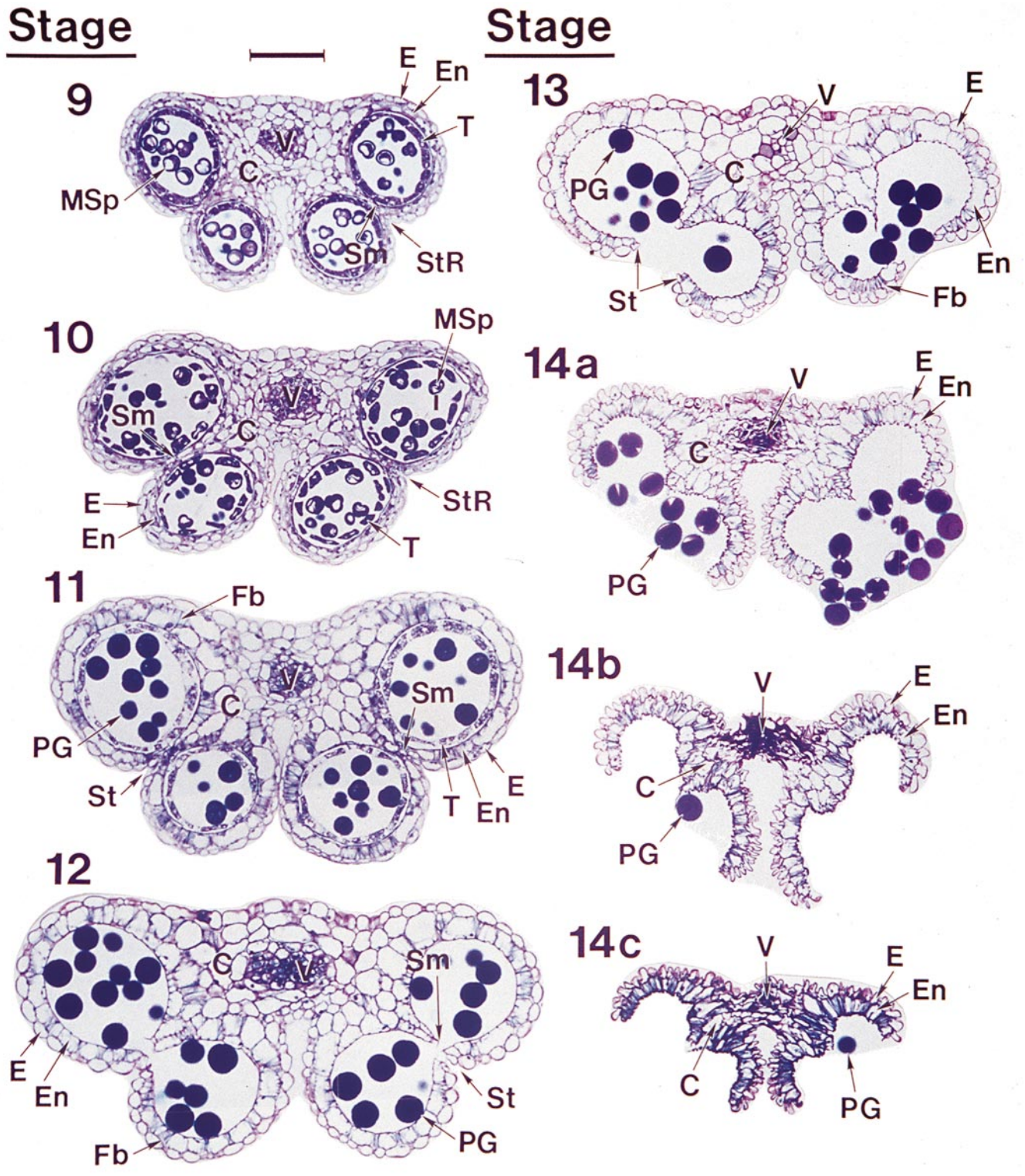

Fig. 4 Phase two of wild-type *Arabidopsis thaliana* anther development. Flowers were fixed and embedded in LR-White plastic resin and sliced into 1 μm transverse sections as described in Materials and methods. The flower sections were stained in toluidine blue and anthers were photographed by bright-field microscopy. Stages 9 to 11, 12 to 13, and 14a to 14c represent anther late development, dehiscence, and senescence, respectively. *C*, connective; *E*, epidermis; *En*, endothecium; *Fb*, fibrous bands; *MSp*, microspores; *PG*, pollen grains; *Sm*, septum; *St*, stomium; *StR*, stomium region; *T*, tapetum; *V*, vascular region. *Bar*=50 μm and applies to all stages 9–14c

visible changes in specific anther cell types that preceded the release of pollen grains during dehiscence (Fig. 4, stage 13). Table 5 summarizes the major events that occurred during the dehiscence program. These included expansion of the endothecium layer, deposition of fibrous bands (wall thickenings) in endothecial and connective cells, and the disappearance of the tapetum and middle layers (Fig. 3 and Fig. 4, stages 7 to 11). Finally, the degeneration of the septum during stages 11 and 12

Table 4 Major events during *Arabidopsis* anther development[a]

Anther stage	Major events and morphological markers[b]	Tissues present[c]	Flower stage[d]	Pollen stage[e]
1	Rounded stamen primordia emerge	L1, L2, L3	5	
2	Archesporial cells arise in four "corners" of L2 layer. Change in shape of primordia to more oval.	E, Ar		
3	Four regions of mitotic activity. 1° parietal and 1° sporogenous layers derived from archesporial cells. Further divisions of each layer generate the 2° parietal layers and sporogenous cells, respectively.	E, 2°P, Sp	7	
4	Four-lobed anther pattern with two developing stomium regions ("notch") generated. Vascular region initiated.	E, En, ML, T, Sp, C, V	8	
5	Four clearly defined locules established. All anther cell types present and pattern of anther defined. Microspore mother cells appear.	E, En, ML, T, MMC, C, V	9	3
6	Microspore mother cells enter meiosis. Middle layer is crushed and degenerates. Tapetum becomes vacuolated and the anther undergoes a general increase in size.	E, En, ML, T, MC, C, V		
7	Meiosis completed. Tetrads of micropsores free within each locule. Remnants of middle layer present.	E, En, ML, T, Tds, C, V		4
8	Callose wall surrounding tetrads degenerates and individual microspores released.	E, En, T, MSp, C, V	10	5
9	Growth and expansion of anther continue. Microspores generate an exine wall and become vacuolated. Septum cells can be distinguished at the level of the TEM. [f]	E, En, T, MSp, C, V, Sm		6–7
10	Tapetum degeneration initiated.	E, En, T, MSp, C, V, Sm	11–12	
11	Pollen mitotic divisions occur. Tapetum degenerates. Expansion of endothecial layer. Secondary thickenings or "fibrous bands" appear in endothecium and connective cells. Septum cell degeneration intiated. Stomium differentiation begins.	E, En, T, PG, C, V, Sm, St		8–9
12	Anther contains tricellular pollen grains. Anther becomes bilocular after degeneration and breakage of septum below stomium. Differentiated stomium seen in TEM. [f]	E, En, PG, C, V, St		10
13	Dehiscence. Breakage along stomium and pollen release.	E, En, PG, C, V	13–14	
14	Senescence of stamen. Shrinkage of cells and anther structure.	E, En, C, V	15–16	
15	Stamen falls off senescing flower.		17	

[a] Anther stages are shown in Figs. 3 and 4

[b] The differentiation of the cell-types within each locule of the anther was not synchronized during stages 1 to 4 (Fig. 3). During this period the locules varied with respect to specific L2-derived cells that they contained. For example, the stage 3 anther shown in Fig. 3 has 1° parietal and 1° sporogenous cells in one locule and 2° parietal and sporogenous cells in another. From stage 5 onwards development of locule cell types was consistent within an anther (Figs. 3 and 4)

[c] *Ar*, archesporial; *C*, connective; *E*, epidermis; *En*, endothecium; *L1*, *L2*, and *L3*, the three cell layers of the stamen primordia; *MC*, meiocyte; *ML*, middle layer; *MMC*, microspore mother cell; *MSp*, microspore; *2°P*, secondary parietal layer; *PG*, pollen grains; *Sm*, septum; *Sp*, sporogenous cells; *St*, stomium; *T*, tapetum; *Tds*, tetrads; *V*, vascular

[d] Flower development stages taken from Smyth et al. (1990) and Bowman et al. (1991)

[e] Pollen development stages taken from Regan and Moffatt (1990)

[f] Transmission electron microscope

generated a bilocular anther (Fig. 4), which was followed by stomium cell breakage and pollen release from the locules during stages 12 and 13 (Fig. 4). Following dehiscence, the anther senesced and fell off the plant with the stamen and rest of the flower (Table 4; Fig. 4, stages 14a to 14c).

undeveloped anther affects early anther development

We examined transverse sections of *undeveloped anther* stamens and identified a range of anther phenotypes (Fig. 5). In most cases (>95%), the stamen consisted of a filament-like structure with an abnormal "swelling" at

Table 5 Dehiscence program in *Arabidopsis* wild-type and mutant anthers[a]

Anther stage[b]	Wild type	*non-dehiscence1* [c]	*delayed-dehiscence1* [c]
11	Expansion of endothecial cell layer and appearance of fibrous bands in endothecium and connective.	Expansion of endothecial cell layer. Distortion of endothecium and connective cells. No fibrous bands observed.	Expansion of endothecial cell layer and appearance of fibrous bands in endothecium and connective.
12	Break in septum below stomium creates bilocular anther.	Endothecium begins to degenerate, including septum.	Break in septum below stomium.
13	Break at stomium in anther wall. Anther wall "flips" back and pollen released during dehiscence.	Anthers do not dehisce. Endothecium degenerated. Pollen appears wild type	Anthers do not dehisce. Pollen storage bodies visible.
Late 13	Pollen grains come in contact with stigmatic papillae. Pollen germination and pollen tube growth in pistil.	In older flowers anthers do not dehisce, pollen appears wild type, and connective degenerates.	In older flowers anthers have not dehisced. Pollen appears to degenerate.
14	Floral organs begin to senesce, the anther shrinks, and cells distort.	Senescence initiated; degeneration of connective and endothecium leaves only vascular bundle and an epidermis surrounding pollen grains. Anthers do not dehisce.	Senescence initiated. Anthers dehisce and pollen degenerates.

[a] Modeled after events described by Keijzer (1987); [b] Refers to anther developmental stages described in Fig. 4 and Table 4
[c] Anther cross-sections for *non-dehiscence1* and *delayed-dehiscence1* are shown in Fig. 8

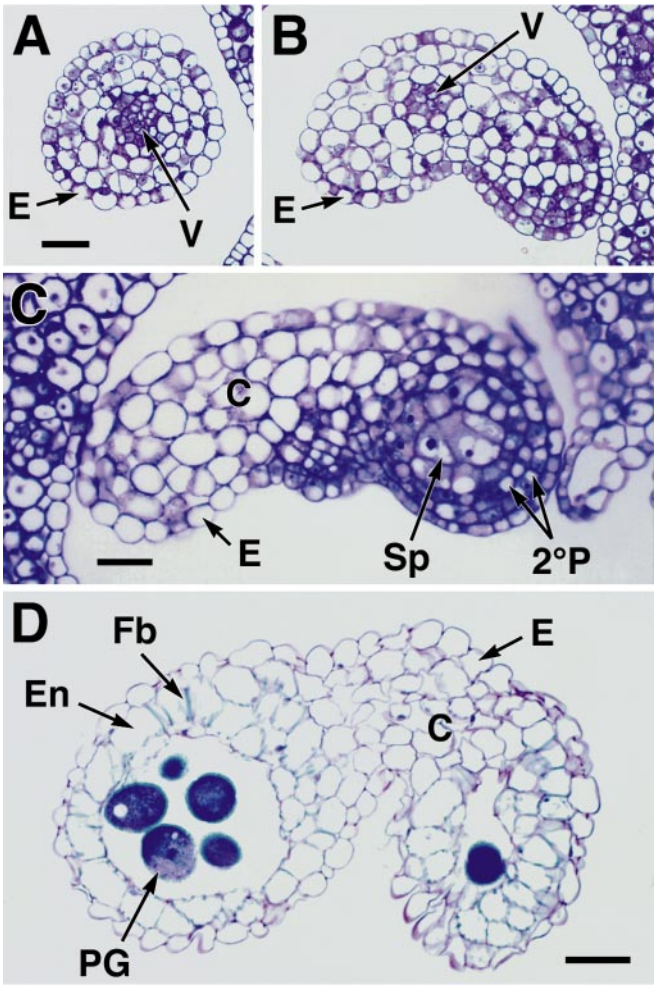

the tip (Fig. 1E and Fig. 2C). The degree of tip "swelling" varied from stamen to stamen (data not shown). The cellular organization of these filament-like structures resembled that of filaments present in wild-type stamens (Fig. 5A and data not shown). An outer layer of epidermal cells was visible that surrounded several rows of parenchymal cells with a vascular bundle within the center (Fig. 5A; Mauseth 1988). The "tip-swelling," on the other hand, did not have an internal tissue organization similar to a wild-type anther at any developmental stage (Fig. 5B). The structure was approximately bilateral in shape, but, with the exception of epidermal, connective-like parenchyma, and vascular cells, did not contain the

Fig. 5A–D Bright-field photographs of anther development in the *undeveloped anther* mutant. Flowers were fixed, embedded in Spurr's epoxy resin, and sliced into 1 μm transverse sections as described in Materials and methods. Sections were stained with toluidine blue and then photographed using bright-field microscopy. Most *undeveloped anther* stamens (>95%), lacked anthers and contained only filament-like structures with terminal "swellings". Labels indicate cell types that were morphologically similar to their counterparts in wild-type anthers. **A** Transverse section through an *undeveloped anther* filament-like structure from a stamen in an open flower (wild-type stage 13). **B** Transverse section through the terminal "tip swelling" of an *undeveloped anther* stamen in an open flower (wild-type stage 13). **C** Transverse section through a rare abnormal anther of an *undeveloped anther* stamen at about wild-type anther stage 4. **D** Transverse section through a rare abnormal anther of an *undeveloped anther* stamen at about wild-type anther stage 12. *C*, connective; *E*, epidermis; *En*, endothecium; *Fb*, fibrous bands; *2°P*, secondary parietal cell layers; *PG*, pollen grain; *Sp*, sporogenous cells; *V*, vascular region. *Bar* in (**A**)=20 μm and represents the same scale in (**B**); *Bar* in (**C**)=20 μm; *Bar* in (**D**)=100 μm

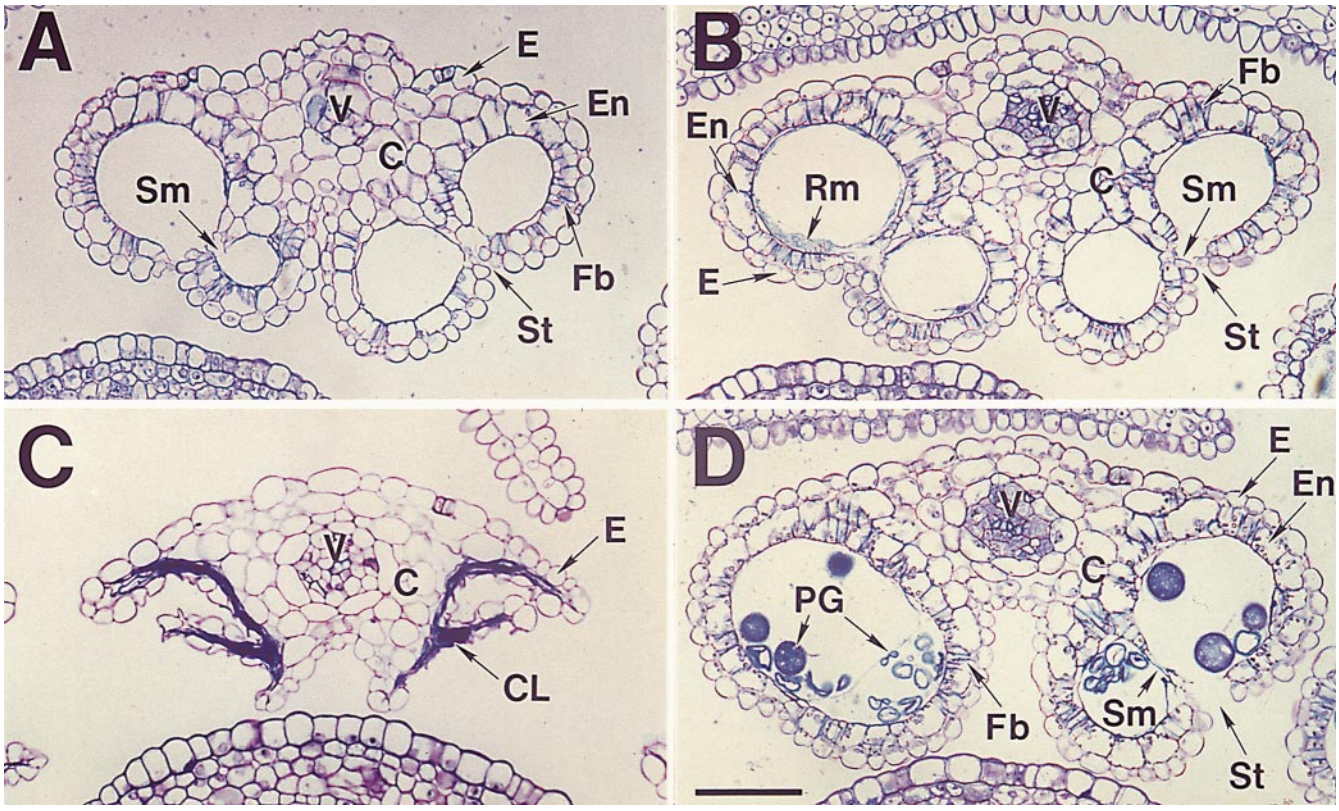

Fig. 6A–D Stage 12 anthers from flowers of *Arabidopsis thaliana* pollenless and defective-pollen mutants. Male-sterile flowers were fixed, embedded in Spurr's epoxy resin, and sliced into 1 μm transverse sections as described in Materials and methods. The flower sections were stained with toluidine blue and anthers were photographed by bright-field microscopy. Transverse sections of stage 12 male-sterile anthers. **A** *pollenless1-1*, **B** *pollenless3-2*, **C** *fat tapetum*, **D** *defective-pollen3*. *C*, connective; *CL*, collapsed locule; *E*, epidermis; *En*, endothecium; *Fb*, fibrous bands; *PG*, pollen grain; *Rm*, remnants of locule contents; *Sm*, septum; *St*, stomium; *V*, vascular region. *Bar*=50 μm.

specialized reproductive and non-reproductive cell types present in a wild-type anther (Fig. 3 and Fig. 4). Occasionally (<5% of the time) *undeveloped anther* stamens developed abnormal anther-like structures that replaced the "tip swellings." Within these structures we observed the development of locules with associated sporogenous cells and wall layers, connective, and vascular regions similar to those in wild-type anthers (Fig. 5C). Typically, however, only two locules were observed in these anthers (Fig. 5C). The sporogenous cells within the anther-like structures were capable of undergoing meiosis and differentiating into functional pollen grains which were released at dehiscence (Fig. 5D and data not shown). Together, these results suggest that *undeveloped anther* plays a role in early anther development, either directly or indirectly, after the stamen primordia specify filament and potential anther regions.

Anther cell processes are affected after microspore mother cell formation in representative pollenless and defective-pollen mutants

We identified a large number of pollenless and defective-pollen mutants in both our T-DNA and EMS mutagenesis screens (Tables 1 and 2). Transverse sections of stage 12 mature anthers from several of these mutants suggested that the mutations targeted either reproductive cells within the locule (e.g., sporogenous cells) or accessory cell layers surrounding the locule (e.g., tapetum, endothecium) or both (Fig. 6). Other cell types in the mutant stage 12 anthers were unaffected (Fig. 6).

Anthers of the *pollenless1–1* mutant (Fig. 6A) and the *pollenless3–2* mutant (Fig. 6B), for example, were indistinguishable from those of wild-type at stage 12 (Fig. 4), except that their locules were either empty (*pollenless1–1*) or contained minor remnants of cell debris (*pollenless3–2*). Other anther tissues, including the epidermis, connective, endothecium, and vascular bundle were not affected (Fig. 6A, B). In addition, septum and stomium cells that participate in the dehiscence process (Fig. 4 and Table 4) were also present (Fig. 6A, B). By contrast, the debris-filled locules of another pollenless mutant, *fat tapetum* (Table 3), were collapsed at stage 12 and the surrounding walls lacked an endothecium layer (Fig. 6C). Other *fat tapetum* tissue layers, such as the epidermis and connective, were similar to those in wild-type anthers at stage 12 (Fig. 4 and Fig. 6C). *defective-pollen3* stage 12 anthers, on the other hand, were not detectably different from those of wild-type plants (Fig. 4)

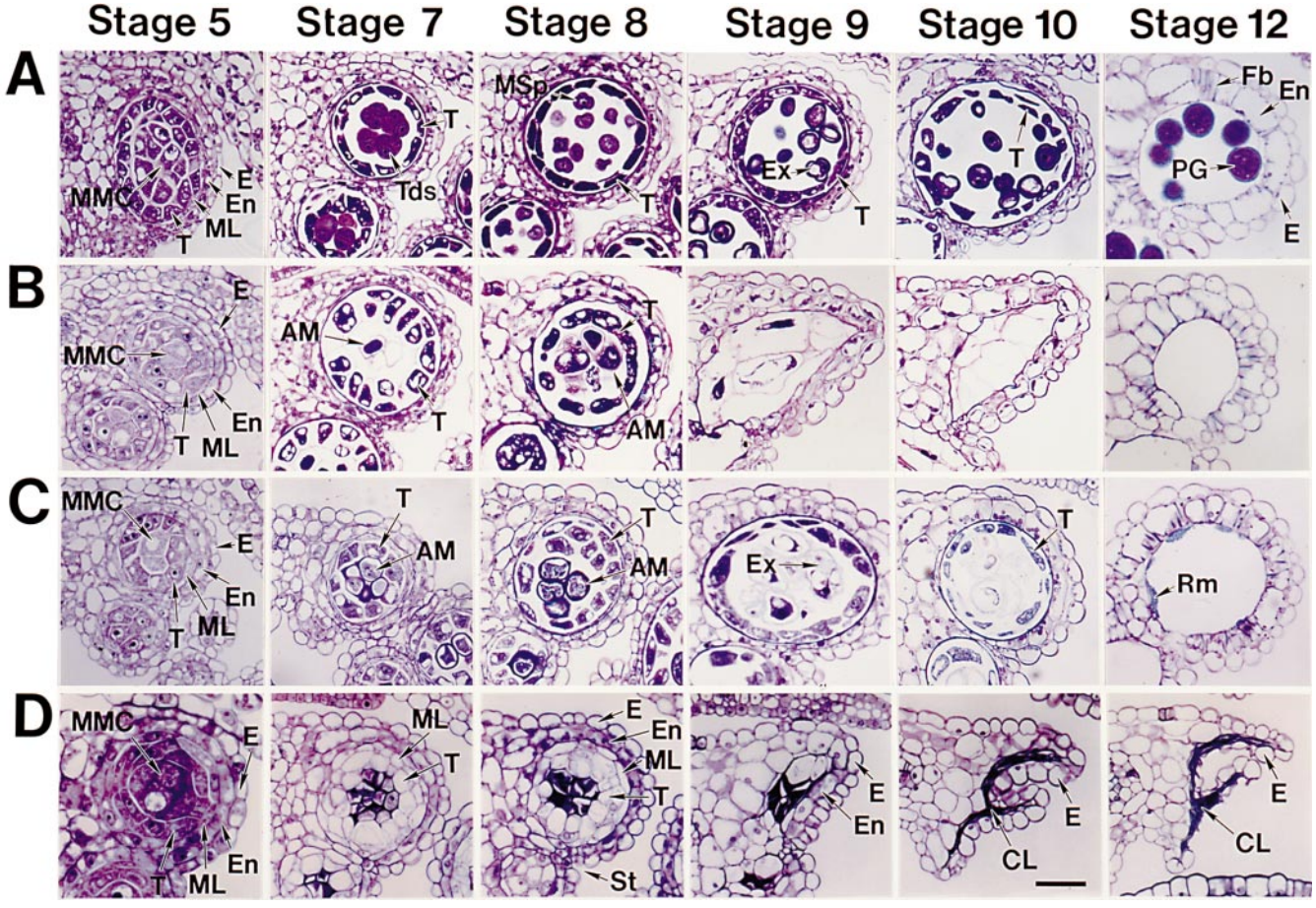

Fig. 7A–D Bright-field photographs of *Arabidopsis thaliana* wild-type and pollenless-class anther development. Flowers were fixed and embedded in either Spurr's or LR-White plastic resins and sliced into 1 μm transverse sections as described in Materials and methods. Flower sections were stained with toluidine blue and anther locules were photographed by bright-field microscopy. **A** Locules from wild-type *Arabidopsis* anthers at stages 5, 7, 8, 9, 10, and 12. **B** Locules from *pollenless1-1* anthers at the same stages of development shown for wild-type anthers (**A**). **C** Locules from *pollenless3-2* anthers at the same stages of development shown for wild-type anthers (**A**). **D** Locules from *fat tapetum* anthers at the same stages of development shown for wild-type anthers (**A**), except that the locule shown in stage 9 was from an early stage 10 anther. *AM*, aberrant material; *CL*, collapsed locule; *E*, epidermis; *En*, endothecium; *Ex*, exine; *Fb*, fibrous bands; *ML*, middle layer; *MMC*, microspore mother cells; *MSp*, microspores; *PG*, pollen grain; *Rm*, remnants of locule contents; *St*, stomium; *T*, tapetum; *Tds*, tetrads. *Bar*=25 μm

and the *pollenless1–1* and *pollenless3–2* mutants (Fig. 6A, B), except that defective pollen-grain-like material was present in the locules (Fig. 6D). The stage 12 anthers of other defective-pollen mutants (e.g., *defective-pollen2*; Table 3) looked similar to those of *defective-pollen3* (data not shown).

We examined transverse anther sections of several pollenless and defective-pollen mutants at different developmental stages to (1) determine when the mutant phenotype was first detectable and (2) identify what cell types were affected by the mutations (Fig. 7). All mutants investigated underwent events similar to those of wild-type during stages 1 to 5 of anther development (Fig. 3 and Table 4; mutant data not shown) and, at stage 5, were indistinguishable from wild-type anthers (Fig. 7A). For example, *pollenless1–1* (Fig. 7B), *pollenless3–2* (Fig. 7C), *fat tapetum* (Fig. 7D), and *defective-pollen3* (data not shown) contained normal-looking microspore mother cells surrounded by a tapetum, middle layer, and endothecium that were not detectably different from those in wild-type anthers (Fig. 3 and Fig. 7A). By contrast, the anthers of each mutant investigated deviated from wild-type after stage 5 when the microspore mother cells entered meiosis (stage 6, Table 4), and by stage 7 lacked normal tetrads (Fig. 7A) and had distinctive mutant phenotypes (Fig. 7B, C, D; *defective-pollen3* data not shown). Although our studies were not detailed enough to pinpoint the precise meiotic stage that was affected in each mutant investigated, others showed recently that *pollenless3* undergoes a third meiotic division without chromosome duplication (*tdm1*; Ross et al. 1997), whereas *defective-pollen3* generates fragmented chromosomes and micronuclei during meiosis (*mei1*, He et al. 1996; *mcd1*, Ross et al. 1997).

Following stage 7, and throughout phase two of anther development (stages 8–14, Table 4), *defective-pollen3* anthers developed similarly to those of wild type (Fig. 4 and Fig. 7A), underwent a normal dehiscence process, and released abnormal pollen grains (Fig. 6D and data not shown). By contrast, we observed three dif-

ferent developmental patterns during phase two for the pollenless mutants investigated (Fig. 7B, C, D). First, in *pollenless1–1* (Fig. 7B) and *pollenless2* (Table 3, data not shown) both the tapetum and abnormal meiotic products contributed to the degenerating cell debris observed within the locules at stages 9 and 10 (Fig. 7B). The tapetum degenerated prematurely in both of these mutants during stages 7 to 9 (Fig. 7B) as compared with the tapetum in wild-type anthers which degenerated after stage 10 (Fig. 4 and Fig. 7A). Second, in *pollenless3–2* (Fig. 7C), *pollenless3–1* (Table 3, data not shown), and *pollenless1–2* (Table 3, data not shown), only the defective meiotic products degenerated in the locules prematurely during stages 9 and 10. The tapetum in these mutants persisted, exine wall material was deposited in the mutant locules, and the tapetum degenerated after stage 10 in a manner similar to that which occurred in wild-type anthers and left remnant material within the locules at stage 12 (Fig. 7A, C). This suggested that the tapetal cell layer in *pollenless3–2*, *pollenless3–1*, and *pollenless1–2* was functional, at least in part. We presume that the difference in *pollenless1–1* (Fig. 7B) and *pollenless1–2* (Table 3, data not shown) tapetal degeneration events was caused by differing strengths of these alleles, *pollenless1–1* being stronger than *pollenless1–2*. Pollenless mutants displaying both of these developmental patterns underwent a normal dehiscence process (Fig. 6A, B and Fig. 7B, C), indicating that neither pollen grains nor tapetal cells play a role in release of pollen from the anther at flower opening (Table 4).

Finally, the *fat tapetum* mutant displayed a third pollenless developmental pattern during phase two of anther development (Fig. 7D). In wild-type anthers the middle layer degenerated during meiosis and by stage 7 was observed only as a crushed remnant between the tapetal and endothecial cell layers (Table 4; Fig. 3 and Fig. 7A). By contrast, the *fat tapetum* middle layer persisted and, together with the tapetum, enlarged significantly at the onset of meiosis and "crushed" the meiotic products within the locules (Fig. 7D, stages 5 to 8). Whether these products were the result of a normal or abnormal meiosis could not be determined with certainty using the anther sections shown here. The enlarged middle and tapetal layers, along with the meiotic products in the locule, degenerated at approximately the same stage that the tapetum degenerated in wild-type anthers (stage 10; Fig. 7A, B). However, these events were followed by abnormal degeneration of the endothecium resulting in a collapse of the *fat tapetum* anther walls by stage 12 (Fig. 6C and Fig. 7D).

Together, these data show that the pollenless and defective-pollen mutants studied here affect anther processes after the differentiation of most anther cell types during phase one of anther development and cause defects in meiosis and/or events that occur in surrounding layers of the locule.

Dehiscence mutants affect stomium breakage late in anther development

We obtained a large number of mutants in both our T-DNA and EMS mutagenesis screens that had defects in the anther dehiscence process (Tables 1 and 2). In our large EMS screen, designed to uncover a range of defective-dehiscence phenotypes, approximately one-third of all male-sterile mutants detected had defects in the dehiscence process (Table 2). These mutants included those with anthers that either dehisced late relative to wild-type anthers or did not dehisce at all (Table 2). In addition, mutants in both dehiscence classes were found that either had pollen or that were pollenless and did not produce detectable amounts of pollen (Table 2). The large majority of dehiscence mutants uncovered in our EMS screen (~53%) had anthers that contained pollen but dehisced late, after the stigma was receptive to successful pollination (Table 2).

We investigated three dehiscence mutants in detail that were obtained from T-DNA Screen 1 (5000 T-DNA; Table 1). These included *delayed-dehiscence1*, *delayed-dehiscence2*, and *non-dehiscence1* which belonged to different complementation groups (Table 3). We examined anthers contained within both mutant and wild-type flowers late in floral development to determine when, or if, anther dehiscence occurred in these mutants. Wild-type anther dehiscence occurred just before or at the time of flower opening (Fig. 1A). By contrast, *delayed-dehiscence1* anthers (Fig. 1D and Fig. 2F) and *delayed-dehiscence2* anthers (data not shown) did not dehisce at flower opening. Both *delayed-dehiscence1* and *delayed-dehiscence2* anthers eventually dehisced, but did so when the pistil was senescing and not receptive to pollen (data not shown). *non-dehiscence1* anthers also did not dehisce at flower opening (data not shown). Unlike *delayed-dehiscence1* and *delayed-dehiscence2* anthers, *non-dehiscence1* anthers did not dehisce at any stage of flower development, and remained unopened up to the time that senescent flowers dropped from *non-dehiscence1* plants (data not shown).

We dissected pollen grains from *delayed-dehiscence1*, *delayed-dehiscence2*, and *non-dehiscence1* anthers at the time of flower opening (anther stage 13, Table 4) and examined them using DAPI (fluorochrome 4′,6-diamidino-2-phenylindole) nuclear stain (Coleman and Goff 1985). Each mutant produced pollen grains that contained three nuclei and that were indistinguishable from those of wild-type plants (data not shown). This result, and visualization of mutant pollen by SEM (Fig. 2I; data not shown) showed that the pollen grains of each mutant were tricellular and had a normal morphology. We determined that the pollen of *delayed-dehiscence1* was functional by collecting seeds from rare expanded siliques found on mutant plants. All of the progeny obtained from these seeds (>50) produced plants with the *delayed-dehiscence1* phenotype. In addition, we were able to generate successful crosses using pollen dissected from *non-dehiscence1* anthers. Together, these results in-

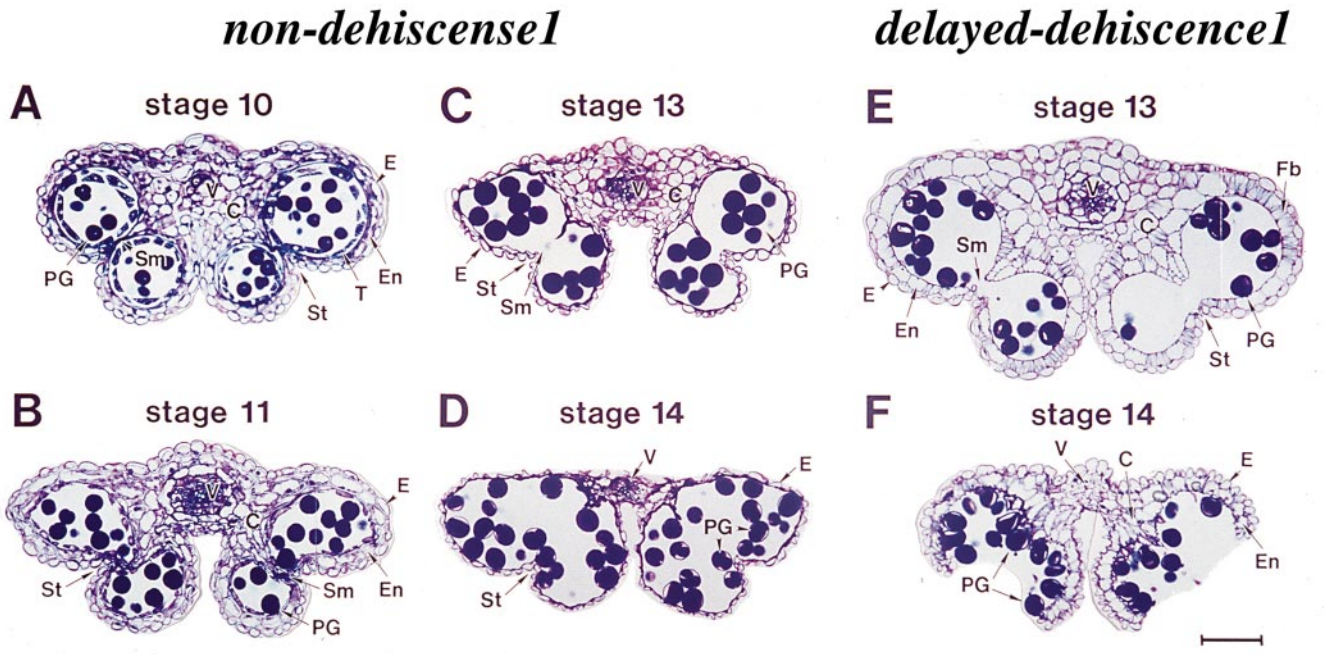

Fig. 8A–F Dehiscence and senescence of *non-dehiscence1* and *delayed-dehiscence1* anthers. Flowers from each mutant were fixed, embedded in LR-White plastic resin, and sliced into 1 μm transverse sections as described in Materials and methods. Flower sections were stained in toluidine blue and anthers were photographed by bright-field microscopy. **A–D** Transverse sections of *non-dehiscence1* anthers: (**A**) stage 10, (**B**) stage 11, (**C**) late-stage 13, (**D**) Stage 14. **E–F** Transverse sections of *delayed-dehiscence1* anthers: (**E**) stage 13, (**F**) stage 14. *C*, connective; *E*, epidermis; *En*, endothecium; *Fb*, fibrous bands; *PG*, pollen grain; *Sm*, septum; *St*, stomium; *T*, tapetum; *V*, vascular region. *Bar*=50 μm

dicated that pollen development was normal in the *delayed-dehiscence1*, *delayed-dehiscence2*, and *non-dehiscence1* mutants.

We examined transverse sections of *delayed-dehiscence1* and *non-dehiscence1* anthers at different developmental stages to investigate the dehiscence defects at the cellular level. No differences were observed in the development of *delayed-dehiscence1* and *non-dehiscence1* anthers when compared to development of wild-type anthers during phase one of anther development (Fig. 3; data not shown). By contrast, development of both *delayed-dehiscence1* and *non-dehiscence1* anthers deviated significantly from that of wild-type anthers (Fig. 4) during late phase two of anther development (Fig. 8; Table 5). *non-dehiscence1* anthers entered the dehiscence program as indicated by endothecial cell expansion and the degeneration of the septum region (Fig. 8A). Late in anther development, however, cells within *non-dehiscence1* anthers underwent a striking cell-death program (Fig. 8B–D). In contrast with wild-type anthers (Fig. 4), the endothecium and connective degenerated completely, resulting in a bilocular anther filled with pollen grains surrounded by a thin epidermal layer. Breakage of the *non-dehiscence1* stomium region within the epidermal layer did not occur (Fig. 8D).

In contrast to *non-dehiscence1*, *delayed-dehiscence1* anthers underwent a dehiscence program similar to that observed in wild-type anthers (Fig. 4 and Fig. 8E, F; Table 5). Endothecial cells expanded, fibrous bands were deposited in the connective and endothecium, septum degeneration occurred, and the stomium broke, releasing viable pollen grains (Fig. 8E, F; Table 5). Breakage of the stomium, however, was delayed in *delayed-dehiscence1* anthers relative to that in wild-type anthers (Table 5). By the time the *delayed-dehiscence1* stomium broke, pollen grains contained within the mutant anthers had begun to degenerate (Fig. 8F). The dehiscence program in *delayed-dehiscence2* anthers was similar to that observed in *delayed-dehiscence1* (data not shown).

Together, these results indicated that the dehiscence program can be interrupted either directly by delaying the timing of stomium breakage (*delayed-dehiscence1*, *delayed-dehiscence2*) or indirectly as a by-product of an abnormal cell-death program (*non-dehiscence1*).

Insertion and deletion alleles identified the *POLLENLESS3* gene

We utilized the *pollenless3–1* and *pollenless3–2* mutant alleles uncovered in our T-DNA Screen 1 (5000 T-DNA, Table 1) to begin to identify and study the genes responsible for the male-sterile phenotypes reported in this paper. We used DNA gel blots with T-DNA right border (RB) and left border (LB) probes (see Materials and methods) to show that the *pollenless3–1* mutant population contained two independently segregating T-DNA inserts, only one of which conferred kanamycin resistance and co-segregated with the *pollenless3–1* mutant phenotype (data not shown). Analysis of the RB and LB T-DNA gel blots indicated that the co-segregating T-DNA in the *pollenless3–1* genome consisted of a simple RB-RB dimer (Fig. 9A, data not shown). The *pollenless3–2* mutant population also contained a T-DNA insert. How-

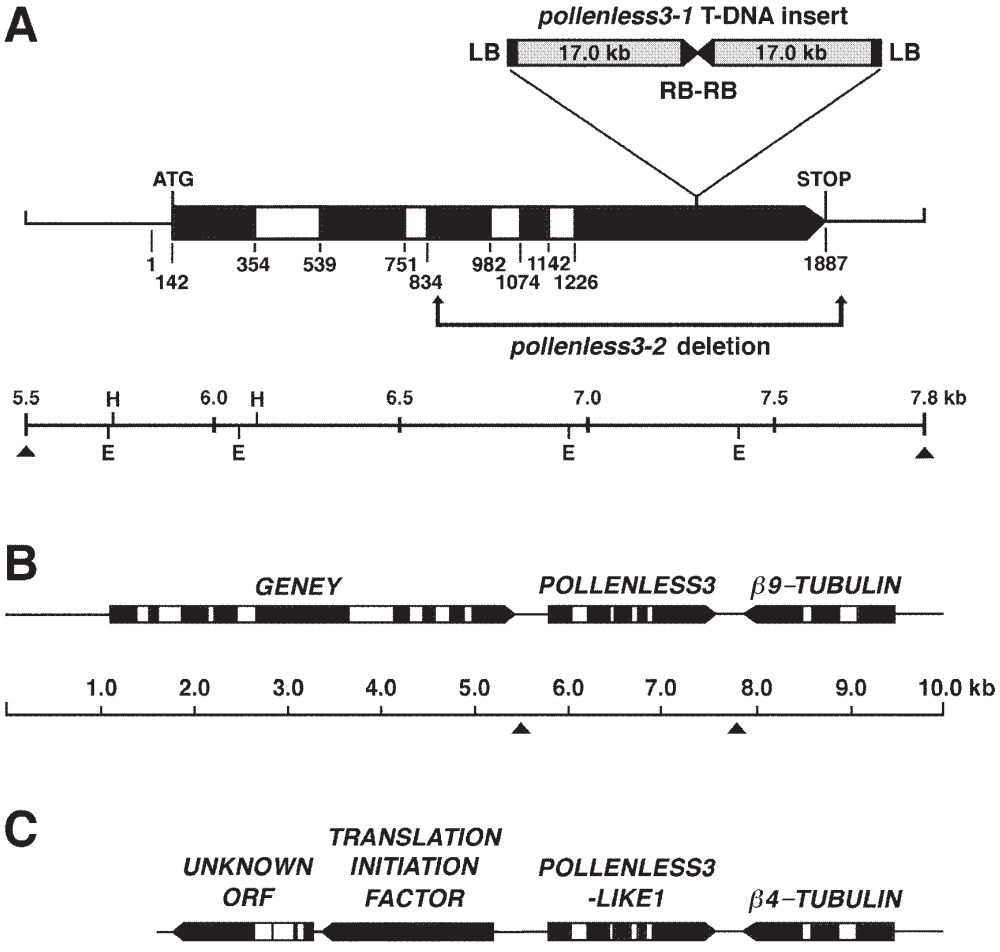

Fig. 9A–C Schematic representation of the *POLLENLESS3* and *POLLENLESS3-LIKE1* gene regions in the *Arabidopsis thaliana* genome. **A** The *pollenless3*, *pollenless3-1*, and *pollenless3-2* alleles. The *solid blocks* delineate the amino acid coding sequence including the ATG, exon-intron junctions, and STOP codon. The *open blocks* represent introns. The *numbers* start from the first upstream nucleotide identified in a partial cDNA sequence (5′ RACE product) and delineate the first and last nucleotide of each exon. The first nucleotide of the ATG start codon and the last nucleotide of the stop codon are also indicated. The T-DNA was inserted into exon 5. The region of a 1-kb (1061-bp) deletion in the *pollenless3-2* allele is indicated by the bracket. The deletion began at the start of exon 3 (7-bp from intron-exon junction) and continued to 14-bp past the STOP codon. A small 64-bp insertion within the deletion site was identified that has homology with the *POLLENLESS3* gene at the 5′ side of the insertion. The right border (*RB*) and left border (*LB*) T-DNA probes used to determine the co-segregation of the T-DNA with the mutant phenotype extended from the teminal HindIII region of the T-DNA to the first adjacent HindIII site within the Ti-plasmid (Zambryski et al. 1980). Plant flanking sequences were identified by SalI left-border plasmid-rescue experiments using the pBR322 ampicillin resistance gene contained within the T-DNA (see Materials and methods). **B** Organization of three genes identified in the *POLLENLESS3* genomic region. The coding exons are shown as *solid blocks*. The exact nucleotides at the beginning of the first exon and the end of the last exon for each gene have not been experimentally determined and are shown as *ATG* and *STOP*. The *scale* given for *GENEY* and *POLLENLESS3* indicates the nucleotide sequence contained within the 7894-bp GenBank accession number AF060248. The *scale* for the *β9-TUBULIN* gene is based on the nucleotide sequence contained in the GenBank accession number M84706 for the *Arabidopsis thaliana* ecotype Columbia (Snustad et al. 1992). The *black triangles* represent the region shown in (**A**). **C** Schematic representation of the duplicated region in the *Arabidopsis thaliana* genome containing the *POLLENLESS3-LIKE1* gene. The *solid boxes* represent the amino acid coding sequences and delineate the ATG, exon-intron junctions, and STOP codons. The *UNKNOWN ORF*, *TRANSLATION INITIATION FACTOR*, *POLLENLESS3-LIKE1*, and *β4-TUBULIN* gene sequences were taken from chromosome 5 GenBank accession number AB011475. *E*, EcoRI; *H*, HindIII; *LB*, T-DNA left border terminus: *RB*, T-DNA right border terminus

ever, this T-DNA did not co-segregate with the *pollenless3–2* mutant phenotype (data not shown).

We used LB T-DNA plasmid rescue experiments with *pollenless3–1* DNA and DNA gel blot studies to identify two LB clones that contained different plant flanking DNA sequences (Fig. 9A, see Materials and methods). Each of these plant DNA sequences generated a unique restriction fragment length polymorphism (RFLP) that distinguished *pollenless3–1* and wild-type DNAs (data not shown). In addition, one of these plant flanking DNA sequences (Fig. 9A, left side of T-DNA) also generated an RFLP that distinguished *pollenless3–1*, *pollenless3–2*, and wild-type DNAs (data not shown). By contrast, the other plant flanking DNA sequence (Fig. 9A, right side of T-DNA) did not hybridize with *pollenless3–2* DNA. These data suggested that (1) the same DNA region was

Table 6 Comparison of the *POLLENLESS3* and *POLLENLESS3-LIKE1* genes and translated proteins

	Nucleotide length											Protein
	prom[a]	exon[b] 1	intron	exon 2	intron	exon 3	intron	exon 4	intron	exon[b] 5	cds[c]	Number of amino acids
POLLENLESS3	420	213	184	213	82	149	91	69	83	661	1305	434
POLLENLESS3-LIKE1	420	192	87	213	79	149	75	69	81	787	1410	469
Percent identity	60%	64%	39%	79%	66%	72%	55%	88%	59%	58%	61%	52%

[a] Compared only the 420-nucleotide upstream region from the *POLLENLESS3* ATG to the *GENEY* STOP codon (Fig. 9B)
[b] As defined in this Table, exon 1 begins at the ATG codon and exon 5 ends at the STOP codon
[c] Coding sequence from ATG to STOP codon

Table 7 Comparison of the *POLLENLESS3-β9-TUBULIN* and *POLLENLESS3-LIKE1-β4-TUBULIN* gene regions

	Nucleotide length										Protein
	Intergenic region		prom [a]	exon [b] 1	intron	exon 2	intron	exon [b] 3	cds [c]		Number of amino acids
POLLENLESS3-β9 [d]	265	*β9-tubulin* [f]	277	394	183	270	105	671	1335		444
POLLENLESS3-LIKE1-β4 [e]	385	*β4-tubulin* [g]	277	394	131	270	88	671	1335		444
Percent identity	48%	Percent identity	63%	88%	43%	86%	51%	87%	87%		96%

[a] Compared only 277-nucleotide upstream region from the *β9-TUBULIN* ATG
[b] As defined in this table, exon 1 begins at the ATG codon and exon 3 ends at the STOP codon
[c] Coding sequence from ATG codon to STOP codon
[d] GenBank accession number AF060248 for the *POLLENLESS3-β9-TUBULIN* region
[e] GenBank accession number AB011475 for chromosome 5 contig containing the *POLLENLESS3-LIKE1-β4-TUBULIN* region
[f] GenBank accession number M84706 (Snustad et al. 1992)
[g] GenBank accession number M21415 (Marks et al. 1987)

altered in the *pollenless3–1* and *pollenless3–2* alleles, (2) the *pollenless3–2* allele contained a deletion, and (3) that both the T-DNA and deletion had disrupted the wild-type *POLLENLESS3* gene (Fig. 9A).

We utilized *pollenless3–1* DNA sequences flanking each side of the T-DNA to isolate genomic clones from a library of wild-type DNA (see Materials and methods). Restriction mapping, DNA sequence analysis (data not shown, GenBank accession number AF060248), and RNA gel blot studies using both plasmid rescue clones and the wild-type genomic clones indicated that there were three genes in the *POLLENLESS3* region: *POLLENLESS3*, *β9-TUBULIN* (Snustad et al. 1992), and an unidentified gene that we designated as *GENEY* (Fig. 9B). We isolated cDNA clones corresponding to both *POLLENLESS3* and *GENEY* mRNAs (see Materials and methods), and determined the structures of the *POLLENLESS3* and *GENEY* genes by comparing genomic and cDNA sequences (Fig. 9B). A search of the publically available gene and protein databases did not reveal any known gene related to either *POLLENLESS3* or *GENEY*. Genetic mapping studies by others showed recently that the *POLLENLESS3* gene was present on chromosome 4 (*tdm1*, Ross et al. 1997), in agreement with the mapping location of RFLP markers flanking the *β9-TUBULIN* gene (*Arabidopsis thaliana* Database, http://genome-www.stanford.edu/Arabidopsis).

The *POLLENLESS3* gene consisted of five exons and four introns (Fig. 9A, B; Table 6). The T-DNA inserted into exon five of the *pollenless3–1* allele. We used PCR to obtain a genomic clone of the *pollenless3–2* gene (see Materials and methods). DNA sequencing studies indicated that most of exon 3 and all of exons 4 and 5 were deleted in the *pollenless3–2* allele (Fig. 9A). Together, these data show that we have cloned the *POLLENLESS3* gene and identified the mutations responsible for the *pollenless3* phenotype (Fig. 6B and Fig. 7C).

The *POLLENLESS3* and *β9-TUBULIN* gene region is duplicated in the *Arabidopsis thaliana* genome

Our PCR experiments to delineate the deletion end points of the *pollenless3–2* allele (Fig. 9A) generated two wild-type DNA fragments (1.9 kb and 2.1 kb) using primers from exon 1 of *POLLENLESS3* and exon 3 of *β9-TUBULIN* (Fig. 9B, data not shown; see Materials and methods). We used DNA sequencing studies to show that the 1.9-kb DNA fragment represented the *POLLENLESS3* and *β9-TUBULIN* gene region (Fig. 9B), whereas the 2.1-kb DNA fragment contained sequences related to both the *POLLENLESS3* and *β9-TUBULIN* genes (data not shown). We searched the GenBank and showed that the 2.1-kb DNA fragment shared 100% sequence identity

with part of a contig from chromosome 5 (GenBank accession number AB011475, Marks et al. 1987; Snustad et al. 1992; 60583-bp K9L2 contig, Kaneko et al. 1998), and contained the 3′ end of the *β4-TUBULIN* gene and the 5′ end of a related gene that we designated as *POLLENLESS3-LIKE1* (Fig. 9C). Computer analysis of the *POLLENLESS3-LIKE1* and *β4-TUBULIN* region within the chromosome 5 contig did not reveal any sequences with similarity to *GENEY*, but suggested that the chromosome 4 *POLLENLESS3* and *β9-TUBULIN* genes were duplicated and represented by the *POLLENLESS3-LIKE1* and *β4-TUBULIN* genes on chromosome 5 (Fig. 9B, C).

We compared the *POLLENLESS3-β9-TUBULIN* and *POLLENLESS3-LIKE1-β4-TUBULIN* gene regions on chromosomes 4 and 5 (Fig. 9B, C; Table 6 and Table 7). Each duplicated gene segment shared a high degree of sequence similarity, particularly within exon regions, and had an identical organization of exons and introns (Fig. 9B, C; Table 6 and Table 7). The coding sequences of the *POLLENLESS3* and *POLLENLESS3-LIKE1* genes were 61% identical, whereas those of the *β9-TUBULIN* and *β4-TUBULIN* genes were 87% identitcal (Table 6 and Table 7). DNA gel blot studies at low stringency indicated that other *POLLENLESS3-LIKE* DNA sequences were present in the *Arabidopsis thaliana* genome (data not shown), one of which was represented in the *Arabidopsis thaliana* EST database (GenBank accession numbers H77068 and AF031608, Glover et al. 1998). We designated this EST as *POLLENLESS3-LIKE2*. Together, these studies indicate that the *POLLENLESS3* gene is a member of a small divergent gene family that is present in at least two different locations in the *Arabidopsis thaliana* genome.

The *POLLENLESS3* and *POLLENLESS3-LIKE1* genes are expressed in floral and vegetative organs

We used RNA gel blots (Fig. 10A–C) and RT-PCR (Fig. 10D, E) to determine the expression patterns of the *POLLENLESS3* and *POLLENLESS3-LIKE1* genes during floral and vegetative development. In each case, we utilized polysomal RNAs to ensure that we would detect transcripts that were loaded onto polysomes and which were actively engaged in protein synthesis (Kamalay and Goldberg 1980). We used the *GENEY* and *β9-TUBULIN* genes as a control.

We detected a 1.3-kb POLLENLESS3 mRNA within a mixture of inflorescences at different developmental stages under conditions in which there was no cross-hybridization with POLLENLESS3-LIKE1 transcripts (Fig. 10B, lane 1; see Materials and methods). We were only able to detect the POLLENLESS3 mRNA by using a large amount of poly(A) mRNA (9 μg) and a long autoradiogram exposure time (5 days), indicating that the POLLENLESS3 mRNA was present at a low level within the mixed inflorescence mRNA population (Fig. 10B). POLLENLESS3 mRNA was also found within siliques,

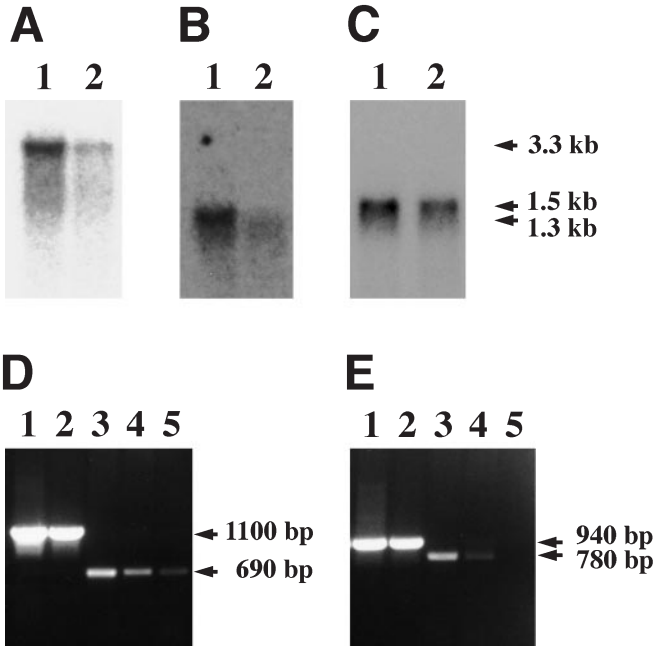

Fig. 10A–E Representation of POLLENLESS3 and POLLENLESS3-LIKE1 mRNAs within *Arabidopsis thaliana* floral and vegetative organs. **A–C** Polysomal poly(A) mRNA was isolated from wild-type organs, size-fractionated by electrophoresis in formaldehyde gels, blotted to nylon filters, and hybridized with ^{32}P-labelled probes (see Materials and methods). *Lanes 1 and 2* contain inflorescence and silique RNAs, respectively. **A** Hybridization with a *GENEY* genomic DNA fragment. Exposure time was 17 h. Inflorescence poly(A) mRNA (9 μg). Silique poly(A) mRNA (3 μg). **B** Hybridization with a *POLLENLESS3* genomic DNA fragment. Exposure time was 5 days. Inflorescence poly(A) mRNA (9 μg). Silique poly(A) mRNA (3 μg). **C** Hybridization with a *β9-TUBULIN* genomic DNA fragment. Exposure time was 17 h. Inflorescence and silique poly(A) mRNAs (1 μg). **D–E** Polysomal poly(A) mRNAs were isolated from wild-type organ systems and gene-specific DNA products were generated using RT-PCR (see Materials and methods). The DNA products in *lanes 1 and 2* were generated using PCR from plasmid and genomic DNAs, respectively. The DNA products in *lanes 3, 4, and 5* were generated using RT-PCR from inflorescence, leaf/stem, and root poly(A) mRNAs, respectively (see Materials and methods). (**D**) *POLLENLESS3*-specific primers. (**E**) *POLLENLESS3-LIKE1*-specific primers

but at a level lower than that observed within inflorescences (Fig. 10B, lane 2). GENEY mRNA (Fig. 10A) and β9-TUBULIN mRNA (Fig. 10C) were also detected in developing inflorescences (Fig. 10A, C, lane 1) and siliques (Fig. 10A, C, lane 2) at levels higher than that observed for POLLENLESS3 mRNA. β9-TUBULIN mRNA was present at the highest level, although under our hybridization conditions we would have detected related β-TUBULIN mRNAs, including β4-TUBULIN mRNA (Table 6 and Table 7).

We used RT-PCR and gene-specific primers to compare *POLLENLESS3* and *POLLENLESS3-LIKE1* expression patterns (Fig. 10D, E). Each primer flanked an intron region so that we could distinguish between unprocessed primary transcripts (Fig. 10D, E, lanes 1, 2) and mRNAs (Fig. 10D, E, lanes 3–5). A 690-bp POLLEN-

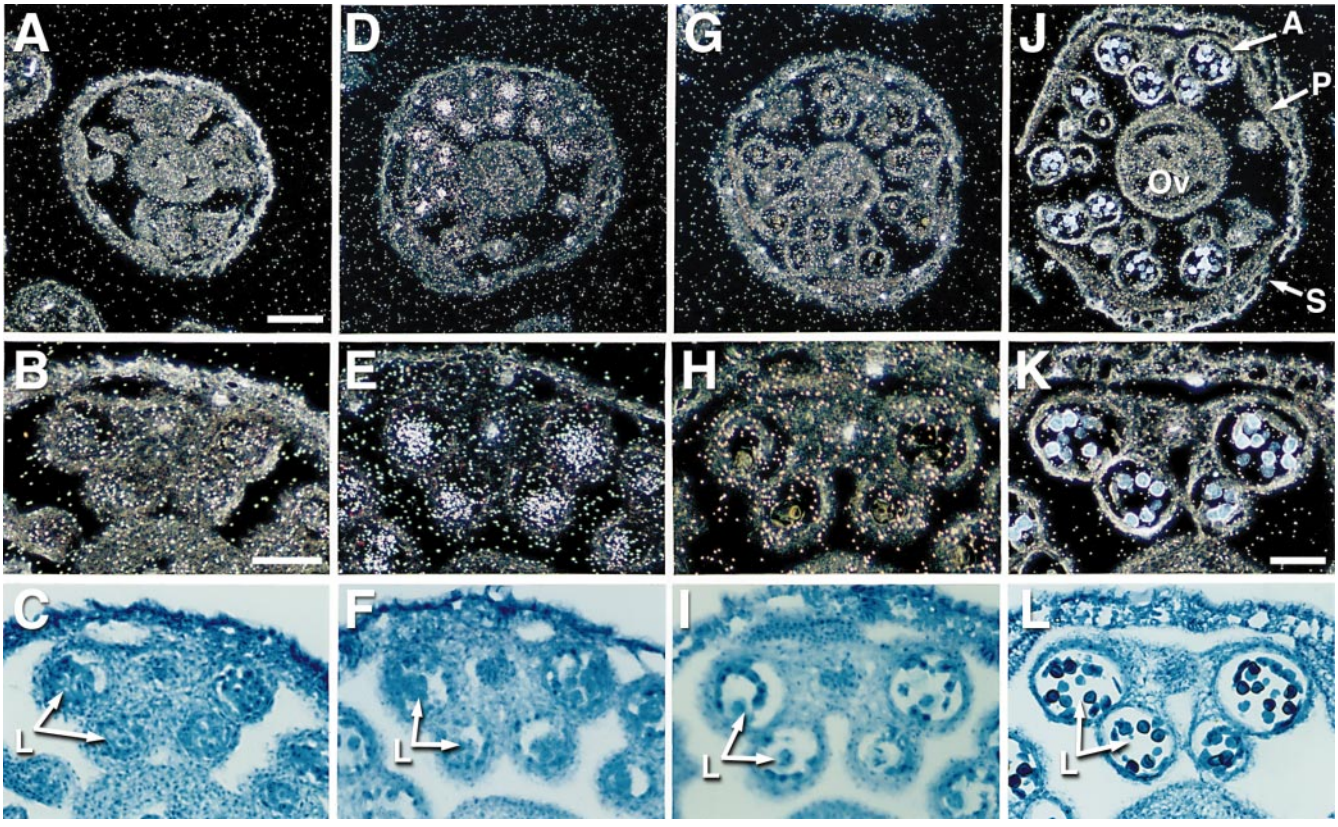

Fig. 11A–L Localization of POLLENLESS3 mRNA within the locules of *Arabidopsis thaliana* wild-type anthers. Inflorescences were fixed, embedded in paraffin, sliced into 10 μm transverse sections, and hybridized with POLLENLESS3 anti-mRNA probes as outlined in Materials and methods. **A**, **B**, **D**, **E**, **J**, **K** Hybridization of a POLLENLESS3 anti-mRNA probe with wild-type anthers before meiosis (stage 5, **A**), during meiosis (stage 6, **D**), and after meiosis (stage 9, **J**). These stages are described in Table 4. **B**, **E**, **K** Higher magnification of (**A**), (**D**), and (**J**). Slide emulsions were exposed for 26 days and the photographs were taken by dark-field microscopy. **G, H** Hybridization of a POLLENLESS3 anti-mRNA probe with *pollenless3-2* mutant anthers during meiosis (stage 6, **G**). A higher magnification of (**G**) is shown in (**H**). Slide emulsions were exposed for 26 days and the photographs were taken using dark-field microscopy. **C**, **F**, **I**, **L** Bright-field photographs of the anthers shown in (**B**), (**E**), (**H**), and (**K**). *A*, anther; *L*, locule; *Ov*, ovary; *P*, petal; *S*, sepal. *Bar* in (**A**)=100 μm and this is the scale for (**D**), (**G**), and (**J**). *Bar* in (**B**)=50 μm and this is the scale for (**C**), (**E**), (**F**), (**H**), and (**I**). *Bar* in (**K**)=50 μm and is the scale for (**L**)

LESS3 RT-PCR product was generated with inflorescence, leaf/stem, and root mRNAs (Fig. 10D, lanes 3–5). By contrast, a 780-bp POLLENLESS3-LIKE1 RT-PCR product was generated with only inflorescence and leaf/stem mRNAs (Fig. 10E, lanes 3, 4). Root mRNA did not generate a POLLENLESS3-LIKE1 RT-PCR product (Fig. 10E, lane 5). Together, these data show that both the *POLLENLESS3* and *POLLENLESS3-LIKE1* genes are expressed in developing floral buds, and that these genes have different expression patterns in vegetative organ systems.

POLLENLESS3 mRNA is localized specifically within anther cells undergoing meiosis

We hybridized a POLLENLESS3 anti-mRNA probe in situ with transverse sections of wild-type inflorescences at different developmental periods to localize POLLENLESS3 mRNA within the developing floral buds (see Materials and methods). We used sections that contained anthers ranging from stages 3 to 10 (Table 4) to monitor *POLLENLESS3* gene expression throughout anther development. POLLENLESS3 mRNA was not detected within stage 3, 4, or 5 anthers prior to when microspore mother cells entered meiosis (Fig. 11A–C, stage 5 and data not shown). Nor was POLLENLESS3 mRNA detected in other developing floral organs during this period (Fig. 11A and data not shown). By contrast, POLLENLESS3 mRNA was observed specifically within meiotically-dividing cells of the locules at stage 6 (Fig. 11D–F). Close inspection of several stage 6 hybridization sections using both bright-field and dark-field microscopy suggested that the POLLENLESS3 mRNA was present within cells late in meiosis (Fig. 11E, F and data not shown). No POLLENLESS3 mRNA was detected within the anther at stages 7 to 10 following meiosis or in any other floral bud region (Fig. 11J–L, stage 9 and data not shown). Hybridization of the POLLENLESS3 anti-mRNA probe with *pollenless3–2* deletion mutant floral bud sections did not produce a hybridization signal above background at any developmental period (Fig. 11G–I), stage 6 and data not shown). Together, these data indicate that the *POLLENLESS3* gene is ex-

pressed transiently during flower development within anther cells undergoing meiosis and that the *POLLENLESS3* expression pattern correlates well with the phenotype produced by the mutant *pollenless3–1* and *pollenless3–2* genes (Fig. 7C).

Discussion

A large number of genes are expressed within the anther

DNA/RNA hybridization studies with RNA populations showed that about 25000 diverse genes are expressed in the tobacco anther at stage 6 (Kamalay and Goldberg 1980), the period during phase two of tobacco anther development when most specialized cell types are still present and the microspore nucleus divides within the locules (Koltunow et al. 1990). Approximately 10 000 of these genes encode mRNA species that are anther-specific and not detectably expressed in other floral and vegetative organs (Kamalay and Goldberg 1980, 1984). The large number of anther-specific genes most likely reflects the complexity of gene expression events required to establish and maintain the differentiated state of highly specialized cells and tissues within the anther (Goldberg et al. 1993). In addition, these genes are required to program novel functional activities that occur within the anther, such as dehiscence and pollen formation (Goldberg et al. 1993). The mechanisms and genes that control the anther-specific gene set both spatially and temporally throughout anther development are not known.

Arabidopsis thaliana anthers differ greatly from those of tobacco in terms of size and cell number, although the types of specialized cells and their spatial organization within the anther are similar (Fig. 3 and Fig. 4; Koltunow et al. 1990). Major cell differentiation and cell degeneration events that occur during phase one and phase two of anther development are also similar in *Arabidopsis thaliana* and tobacco, although minor differences occur particularly in phase two (Fig. 3 and Fig. 4; Koltunow et al. 1990). For example, in *Arabidopsis thaliana* anthers tapetal cell degeneration occurs later, the connective does not degenerate, and fibrous bands are deposited in both the endothecium and connective (Fig. 3 and Fig. 4; Koltunow et al. 1990).

Anther-specific genes like those found in tobacco (Kamalay and Goldberg 1980, 1984) would be expected to have counterparts in *Arabidopsis thaliana*, although they would reflect the minimal anther-specific gene set because of the smaller size of the *Arabidopsis thaliana* genome (120 Mb; Bevan et al. 1998) relative to that of tobacco (1500 Mb; Kamalay and Goldberg 1980). Assuming that there are 60 000 genes in tobacco (Kamalay and Goldberg 1980) and 20 000 genes in *Arabidopsis thaliana* (Bevan et al. 1998), we predict that approximately 8000 genes should be expressed during phase two of *Arabidopsis thaliana* anther development at a stage equivalent to that used in our tobacco gene expression studies (Stage 10, Fig. 4 and Table 4). Of these, we would expect that approximately 3500 genes should be expressed specifically within the *Arabidopsis thaliana* anther. What proteins these genes encode, and what functions they carry out during anther development remain to be determined.

Male-sterile mutants that affect anther sporophytic functions were identified

The *Arabidopsis thaliana* T-DNA and EMS mutagenesis screens we carried out were designed to identify mutants with defects in anther development that result in a male-sterile phenotype. We chose not to investigate sterility mutants that were due to homeotic or non-homeotic floral mutations, even though many of these mutants were identified in both our T-DNA and EMS screens (Table 1 and Table 2). Our goal was to identify male-sterility mutants in which third-whorl floral organ development had been initiated, stamen identity was wild type, and other floral organs were not affected. These mutations would be expected to be downstream of the regulatory genes and processes that control stamen primordia identity (e.g. *AG*, *PI*, *AP3*; Coen and Meyerowitz 1991) and, therefore, would cause defects in the differentiation and/or function of anther cell types.

Because we employed silique expansion as the criterion for the selection of fertility mutants, mutations disrupting anther functions and/or pollen development that did not result in either a reduction in fertility or a male-sterile phenotype would not have been detected in our screens. Mutations in genes that are expressed only within pollen grains during the haploid gametophytic generation would also not have been identified in either our T-DNA or EMS screens. These mutants would be expected to cause a 50% reduction in pollen production and, as such, would not lead to a male-sterile phenotype (Sari-Gorla et al. 1996, 1997; Chen and McCormick 1997). Our screens, therefore, and similar screens carried out by other laboratories (Van Der Veen and Wirtz 1968; Chaudhury et al. 1992; Chaudhury 1993; Dawson et al. 1993; Peirson et al. 1996; Taylor et al. 1998), were designed to detect mutations in sporophytically acting genes that prevent the generation and/or release of pollen grains.

The results of our large EMS mutagenesis screen (Table 2) reflect the complexity and diversity of functions carried out by the anther and, as predicted from our gene expression studies (Kamalay and Goldberg 1980, 1984), indicate that a large number of genes are required to carry out these functions during anther development. We uncovered over 600 mutants, or 5% of the M1 lines screened, that had defects associated with anther development and/or function (Table 2). These included mutants with defects in anther differentiation, establishment of anther morphology, pollen development and/or function, and pollen release at floral opening (Table 2). Although we do not know how many complementation groups are represented within this mutant population, it

is possible that we have generated mutations in a significant fraction (~5–10%) of the genes predicted to be expressed specifically during *Arabidopsis thaliana* anther development. Other researchers have found a large number of *Arabidopsis thaliana* male-sterile mutations, including those that cause defects in (1) meiosis (Aarts et al. 1993; Dawson et al. 1993; Peirson et al. 1996, 1997; Chaudhury et al. 1994a, b; Preuss et al. 1994; He et al. 1996; Hulskamp et al. 1997; Ross et al. 1997; Glover et al. 1996, 1998), (2) post-meiotic pollen development (Taylor et al. 1998; Moffatt and Sommerville 1988; Regan and Moffat 1990), (3) pollen structure and function (Preuss et al. 1993; Aarts et al. 1995), and (4) dehiscence (Dawson et al. 1993; McConn and Browse 1996). Analogous mutations have been identified in other flowering plants such as maize (Albertsen and Phillips 1981; Staiger and Cande 1990, 1993) and tomato (Rick 1948; Gottschalk and Wolff 1983). Clearly, these mutants and those uncovered here represent a rich collection of mutants to uncover genes that play important roles in anther cell processes.

fat tapetum and *undeveloped anther* may be involved in anther cell identity and cell specification processes

We initiated the *Arabidopsis thaliana* mutagenesis screens to attempt to identify mutants that disrupt critical steps in anther development and cell differentiation. To date, there have been no reports of mutant genes that disrupt the differentiation of anther cell types. This is probably due, in part, to the difficulty of identifying mutants that affect anther cell differentiation in large mutant populations without the use of anther-cell-specific marker genes (Koltunow et al. 1990; Goldberg et al. 1993; Beals and Goldberg 1997). On the other hand, it is also possible that genes controlling anther cell differentiation events are duplicated in the genome (Bevan et al. 1998) and/or utilized at other times in the plant life cycle. If so, it would not be possible to identify mutations in these genes using conventional screens.

The *fat tapetum* mutant, which has a phenotype similar to *ms3* (Chaudhury et al. 1994a), affects the functioning of several anther cell types including the tapetum, middle layer, and endothecium (Fig. 7D). All of these cells are derived from the L2 layer of the stamen primordium (Fig. 3; Goldberg et al. 1993). One particularly striking effect is the failure of the *fat tapetum* middle layer to degenerate after meiosis. Instead, the middle layer undergoes a series of cell events identical to that of its neighboring tapetal cell layer (Fig. 7D), suggesting that the middle layer may have become "tapetal-like" in the *fat tapetum* mutant. If so, then the *FAT TAPETUM* gene might play a role in establishing middle layer cell identity after division of the 2° parietal cells early in anther development (Fig. 3). Although speculative, this hypothesis can be tested by using a tapetal-cell-specific reporter gene (e.g. *TA29/GUS*) to establish the identity of the middle layer in the *fat tapetum* mutant (Koltunow et al. 1990; Mariani et al. 1990).

By contrast, *UNDEVELOPED ANTHER* may play a role, either directly or indirectly, in directing anther differentiation events after stamen specification has occurred (Fig. 1B, Fig. 2D, and Fig. 5). Most stamens in *undeveloped anther* flowers have a normal-appearing filament and lack a well-differentiated anther (Fig. 5). The abnormal "swellings" at the tip of a mature *undeveloped anther* stamen do not have the specialized cell types present in anthers at any stage of development (Fig. 5). These results suggest that different genes control the differentiation of the stamen into filament and anther regions, and that *UNDEVELOPED ANTHER* may play a role in the anther differentiation process.

Two other genes, *ETTIN* (Sessions and Zambryski 1995) and *AINTEGUMENTA* (Elliott et al. 1996; Klucher et al. 1996), also appear to play a role in anther development. *AINTEGUMENTA* is an *APETALA2-LIKE* gene that encodes a transcription factor (Elliott et al. 1996; Klucher et al. 1996), whereas *ETTIN* is related to DNA binding proteins that bind to auxin response elements and is probably also a transcription factor (Sessions et al. 1997). Both *ettin* and *aintegumenta* mutants are female sterile, and many *ettin-like* and *ant-like* mutants were uncovered in our EMS screen (Table 2). *ettin* and *aintegumenta* anthers have an altered number of locules, produce functional pollen, and dehisce. This suggests that the *ETTIN* and *AINTEGUMENTA* genes play a role, either directly or indirectly, in establishing locule number during anther development.

Dehiscence mutants either delay or prevent the anther from breaking at the stomium region

Our EMS screen was designed primarily to uncover *Arabidopsis thaliana* mutants in genes that control the dehiscence process, including those involved in stomium cell differentiation and function (Table 2). Recently, we used targeted cell ablation studies to show that a functional stomium is critical in order for dehiscence to occur (Beals and Goldberg 1997). The dehiscence mutants that we studied here produced two different phenotypes (Table 5). *non-dehiscence1* anthers differentiate a normal-looking stomium region, produce viable pollen, but fail to dehisce (Fig 8 E, F). The dehiscence mutant *ms35*/*msH* (Dawson et al. 1993) appears to have a similar phenotype. *non-dehiscence1* anthers undergo a striking cell death program late in phase two that leads to abnormal degeneration of the connective and endothecium (Fig. 8E, F). The failure of *non-dehiscence1* anthers to dehisce could be due to the loss of these cell types rather than to a defect in stomium cell function. For example, loss of the endothecial and connective cells and their associated fibrous bands might reduce mechanical forces required for the anther to "flip open" at dehiscence. Alternatively, loss of these cells might prevent dehiscence program "signals" from reaching their targets in the stomium region.

non-dehiscence1 activates a degeneration program in endothecial and connective cells that does not occur in

wild-type anthers (Fig. 8E, F). One possibility is that *non-dehiscence1* inactivates a cell-death suppression program that operates normally in these cell types and prevents the endothecium and connective from degenerating like the tapetal and middle layers. Defects in cell-death suppression have been identified in *Arabidopsis thaliana* disease resistance lesion-mimics in which cell degeneration is part of the normal hypersensitive response to pathogen attack (Greenberg and Ausubel 1993; Dietrich et al 1997; Gray et al. 1997). It is possible that the cell-death suppression programs in both of these distinct developmental situations occur by common mechanisms.

By contrast, *delayed-dehiscence1* and *delayed-dehiscence2* mutants are defective in the last step of the anther dehiscence program – stomium breakage (Fig. 8A–D and Table 5). These mutants have a normal complement of anther cell types and undergo a dehiscence program. However, breakage of the stomium is delayed relative to that in wild-type anthers (Fig. 4 and Fig. 8A–D; Table 5).

It is possible that the *delayed-dehiscence1* and *delayed-dehiscence2* mutants are defective in a signaling pathway that coordinates the timing of stomium breakage with that of flower opening. *Arabidopsis thaliana* dehiscence mutants have been identified by screens designed to uncover unrelated phenotypes. For example, *coi1* is defective in both pollen development and dehiscence, and was identified by root insensitivity to jasmonic acid (Feys et al. 1994; Dao-Xin et al. 1998). Similarly, the triple *fad* mutant (*fad3–2, fad7–2, fad8*) that was engineered to be deficient in trienoic acid synthesis is also defective in pollen development and release (McConn and Browse 1996). Triple *fad* mutants can be rescued by the application of linolenic acid or jasmonic acid. These results suggest that compounds within the octadecanoic pathway (e.g. jasmonic acid) may perform a signaling function during dehiscence to control the timing of stomium breakage.

POLLENLESS3 is expressed within anther cells undergoing meiosis

Our T-DNA and EMS screens generated a large number of mutant lines with a pollenless phenotype (Table 1 and Table 2). The pollenless mutants investigated here, *pollenless1–1*, *pollenless1–2*, *pollenless3–1*, *pollenless3–2*, and *fat tapetum* appear to have defects in meiotic processes and/or the functioning of accessory cell layers that surround the locules which are required for pollen formation (Fig. 7). Because these mutants have lesions in sporophytically acting genes, those that have meiotic defects must be expressed between the period of microspore mother cell formation and the generation of haploid tetrads (Table 4).

We, and others (Glover et al. 1998), cloned the *POLLENLESS3* gene in the *Arabidopsis thaliana* genome (Fig. 9A). The mutant *pollenless3* alleles affect meiotic events and lead to the production of abnormal tetrad-like structures at stage 7 of anther development (Fig. 7C). Ross et al. (1997) recently showed that meiotic cells in the *pollenless3* (*tdm1*) anthers undergo a third division without DNA replication generating cells with unbalanced chromosome numbers. Our in situ hybridization experiments showed that the POLLENLESS3 mRNA is present only within meiotically-dividing cells of wild-type anthers (Fig. 11). The POLLENLESS3 mRNA accumulates during meiosis after the microspore mother cells begin to divide, is present in dividing cells late in meiosis, and decays prior to the formation of tetrads (Fig. 11). The expression profile of the *POLLENLESS3* gene corresponds well with the observed defects caused by the mutant *pollenless3* alleles (Fig. 7C and Fig. 11D–F; Ross et al. 1997).

The *POLLENLESS3* gene is a member of a small gene family in the *Arabidopsis thaliana* genome represented by at least three members: *POLLENLESS3*, *POLLENLESS3-LIKE1*, and *POLLENLESS3–LIKE2*, all of which are expressed at the mRNA level at some period of development (Fig. 10 and Table 8). Our gene expression studies (Fig. 10 and Fig. 11) showed that the *POLLENLESS3* gene is active in vegetative organ systems (Fig. 10). Inspection of *pollenless3* mutant plants did not reveal any obvious vegetative phenotype. It is possible that the *pollenless3* allele generates a phenotype in vegetative organs too subtle to be identified upon visual inspection. On the other hand, it is also possible that the *pollenless3* gene does not generate a vegetative phenotype because the POLLENLESS3 protein either requires a protein partner for its activity that is absent in vegetative organs or *POLLENLESS3-LIKE* genes compensate for the loss of *POLLENLESS3* function in these organs or both.

What is the function of the *POLLENLESS3* gene? BLAST searches of publicly available gene and protein databases did not produce any statistically significant "hit" to known genes. Detailed analysis of the POLLENLESS3 protein using the UCLA-DOE protein folds server (see Materials and methods) indicated that it consisted primarily of α-helix structural components and contained no significant coiled-coil regions. Searches for functional motifs within the POLLENLESS3 protein revealed the presence of a nuclear localization motif. In addition, clues to the function of the *POLLENLESS3* gene were obtained by the presence of a TPR domain in the POLLENLESS3 protein and in the POLLENLESS3-LIKE proteins as well (Table 8). The TPR domain has been implicated in playing a role in protein-protein interactions and is also present in many eukaryotic proteins, including the *Schizosaccharomyces pombe* rad3 protein and the yeast Cdc23p cell-cycle protein (Table 8). The rad3 protein has been shown to be involved in controlling G2 of the cell cycle (Jimenez et al. 1992), a function consistent with that proposed for the *POLLENLESS3* (*TDM1*) gene (Ross et al. 1997). Taken together, the precise phenotype of the *pollenless3* mutant (Ross et al. 1997), the POLLENLESS3 mRNA localization studies (Fig. 11), and the structural analysis of the POLLEN-

Table 8 TPR motif comparisons between POLLENLESS3 family members and other proteins [a]

POLLENLESS3 [b]	
191–224	ARILGNLGWVHLQLHNYGIAEQHYRRALGLERDK
POLLENLESS3-LIKE1 [c]	
184–217	ARILGNLAWVHLQLHNYGIAEQYYRNALSLEPDN
POLLENLESS3-LIKE2 [d]	
	TRLLGNLGWALMQRDNFVEAEDAYRRALSIAPDN
GMSTI [e]	
m1 [f] 2–35	AEEAKAKGNAAFSAGDFAAAVRHFSDAIALSPSN
m2 69–102	PKAYSRLGAAHLGLRRHRDASPPTKPASNSNPDN
m3 242–275	AQKEKEAGNAAYKKKDFETAIGHYSKALELDDED
m4 381–414	ADEAREKGNELFKQQKYPEATKHYTEAIKRNPKD
m5 415–448	AKAYSNRAACYTKLGAMPEGLKDAEKCIELDPTF
Synechococcus protein [g]	
m1 43–76	LNALLEQGNEQLTNRNFAQAVQHYRQALTLEANN
m2 77–110	ARIHGALGYALSQLGNYSEAVTAYRRATELEDDN
m3 111–144	AEFFNALGFNLAQSGDNRSAINAYQRATQLQPNN
m4 145–178	LAYSLGLATVQFRAGDYDQALVAYRKVLAKDSNN
m5 213–246	AELRIKAAVTWFGLNDRDQAIAFLEEARRLSTRD
S. pombe. rad3 protein [h]	
948–981	AEIYLEIARISRKNGQPQRAFNAILKAMDLDKPL

[a] A repeat structure containing 34 amino acids (*tetratrico*peptide motif) often reiterated within a protein sequence. The TPR domain was first described in a yeast Cdc23p cell-cycle protein (Sikorski et al. 1990). Identified by ProfileScan (see Materials and methods). The conserved amino acids in the TPR motif of the POLLENLESS3 protein family are *underlined*
[b] Encoded by the chromosome *4 POLLENLESS3* gene
[c] Encoded by the chromosome *5 POLLENLESS3-LIKE1* gene
[d] Encoded by the *Arabidopsis thaliana* EST (GenBank accession numbers H77068 and AF031608) that is related to the *POLLENLESS3* and *POLLENLESS3-LIKE1* genes
[e] TPR repeat motif protein from soybean (Hernandez Torres et al. 1995)
[f] Indicates the number of TPR motifs in the protein
[g] 178 NCBI neighbor protein (GenBank accession number 1196960)
[h] *Schizosaccharomyces pombe* rad3 protein has one TPR domain (GenBank accession number 400924)

LESS3 protein (Table 8) strongly suggest that *Arabidopsis thaliana POLLENLESS3* gene encodes a protein that plays a critical role in regulating cell-cycle activity within meiotically-dividing cells in developing anthers.

Acknowledgements We thank Dr. Ken Feldmann for allowing us to screen his T-DNA mutagenized lines, and Drs. Leonore Reiser and Bob Fischer for collaboration on the Arizona screen for fertility mutants. We also thank Dr. Art Gibson for help and use of his SEM, Minh Huynh and Sharon Hue Tu for help with sectioning and microscopy, Weimin Deng and Weigang Yang for their greenhouse assistance, Brandon Hieu Le and Michelle To-Hang Dinh for help with the EMS screen, and Jim Boone who characterized the phenotypes of several mutant lines. We especially thank Birgitta Sjostrand for her expertise and help with the microscopy studies, Margaret Kowalczyk for preparing the figures, and Bonnie Phan for typing the manuscript. We greatly appreciate all the input from Dr. Nickolai Alexandrov for suggestions on computational sequence analysis. This work was funded by an NSF grant to R.B.G., an NIH Postdoctoral Fellowship to T.P.B., and an NZ Grasslands Research Center AgResearch Predoctoral Fellowship to P.M.S.

References

Aarts MGM, Dirkse WG, Stiekema WJ, Pereira A (1993) Transposon tagging of a male sterility gene in *Arabidopsis*. Nature 363:715–717

Aarts MGM, Keijzer CJ, Stiekema WJ, Pereira A (1995) Molecular characterization of the *CER1* gene of *Arabidopsis* involved in epicuticular wax biosynthesis and pollen fertility. Plant Cell 7:2115–2127

Albertsen MC, Phillips RL (1981) Developmental cytology of 13 genetic male sterile loci in maize. Can J Genet Cytol 23: 195–208

Alexandrov NN, Nussinov R, Zimmer RM (1995) Fast protein fold recognition via sequence to structure alignment and contact capacity potentials. In: Hunter L, Klein TE (eds) Pacific symposium on biocomputing 1996. World Scientific Publishing, Singapore, pp 53–72

Altschul SF, Gish W, Miller W, Myers EW, Lipman DJ (1990) Basic local alignment search tool. J Mol Biol 215:403–410

Altschul SF, Madden TL, Schaffer AA, Zhang J, Zhang Z, Miller W, Lipman DJ (1997) Gapped BLAST and PSI-BLAST: a new generation of protein database search programs. Nucl Acids Res 25:3389–3402

Beals TP, Goldberg RB (1997) A novel cell ablation strategy blocks tobacco anther dehiscence. Plant Cell 9:1527–1545

Behringer FJ, Medford JI (1992) A plasmid rescue technique for the recovery of plant DNA disrupted by T-DNA insertion. Plant Mol Biol Rep 10:190–194

Berger B, Wilson DB, Wolf E, Tonchev T, Milla M, Kim PS (1995) Predicting coiled coils by use of pairwise residue correlations. Proc Natl Acad Sci USA 92:8259–8263

Bevan M, et al (1998) The EU *Arabidopsis* genome project. Analysis of 1.9 Mb of contiguous sequence from chromosome 4 of *Arabidopsis thaliana*. Nature 391:485–488

Bowman JL, Smyth DR, Meyerowitz EM (1991) Genetic interactions among floral homeotic genes of *Arabidopsis*. Development 112:1–20

Chaudhury AM (1993) Nuclear genes controlling male fertility. Plant Cell 5:1277–1283

Chaudhury AM, Craig S, Bloemer KC, Farrell L, Dennis ES (1992) Genetic control of male fertility in higher plants. Aust J Plant Physiol 19:419–426

Chaudhury AM, Lavithis M, Taylor PE, Craig S, Singh MB, Signer ER, Knox RB, Dennis ES (1994a) Genetic control of male fertility in *Arabidopsis thaliana*: structural analysis of premeiotic developmental mutants. Sex Plant Reprod 7:17–28

Chaudhury AM, Farrell LB, Chapple R, Bloemer KC, Craig S, Dennis ES (1994b) Genetic and molecular dissection of male-fertility in higher plants. In: Willliams EG, Clarke AE, Knox RB (eds) Genetic control of self-incompatibility and reproductive development in flowering plants. Kluwer, Dordrecht, pp 403–422

Chen YCS, McCormick S (1997) *sidecar pollen*, an *Arabidopsis thaliana* male gametophytic mutant with aberrant cell divisions during pollen development. Development 122:3243–3253

Coen ES, Meyerowitz EM (1991) The war of the whorls: genetic interactions controlling flower development. Nature 353: 31–37

Coleman AW, Goff LJ (1985) Applications of fluorochromes to pollen biology. I. Mithramycin and 4′,6-diamidino-2-phenylindole (DAPI) as vital stains for quantitation of nuclear DNA. Stain Technol 60:145–154

Cox KH, Goldberg RB (1988) Analysis of gene expression. In: Shaw CH (ed) Plant molecular biology: a practical approach. IRL Press, Oxford, pp 1–35

Dao-Xin X, Feys BF, James S, Nieto-Rostro M, Turner JG (1998) *COI1*: An *Arabidopsis* gene required for jasmonate-regulated defense and fertility. Science 280:1091–1094

Dawson J, Wilson ZA, Aarts MGM, Braithwaite AF, Briarty LG, Mulligan BJ (1993) Microspore and pollen development in six male-sterile mutants of *Arabidopsis thaliana*. Can J Bot 71:629–638

Delsney M, Cooke R, Penon P (1983) Sequence heterogeneity in radish nuclear ribosomal RNA genes. Plant Sci Lett 30:107–119

Dietrich RA, Richberg MH, Schmidt R, Dean C, Dangl JL (1997) A novel zinc finger protein is encoded by the *Arabidopsis LSD1* gene and functions as a negative regulator of plant cell death. Cell 88:685–694

Elliott RC, Betzner AS, Huttner E, Oakes MP, Tucker WQ, Gerentes D, Perez P, Smyth DR (1996) *AINTEGUMENTA*, an *APETALA2*-like gene of Arabidopsis with pleiotropic roles in ovule development and floral organ growth. Plant Cell 8: 155–168

Feinberg AP, Vogelstein B (1983) Technique for radiolabelling DNA restriction endonuclease fragments to high specific activity. Anal Biochem 132:6–13

Feldmann KA (1991) T-DNA insertion mutagenesis in *Arabidopsis*: mutational spectrum. Plant J 1:71–82

Feldmann KA, Marks MD (1987) *Agrobacterium*-mediated transformation of germinating seeds of *Arabidopsis thaliana*: a non-tissue culture approach. Mol Gen Genet 208:1–9

Feys BJ, Benedetti CE, Penfold CN, Turner JG (1994) *Arabidopsis* mutants selected for resistance to the phytotoxin coronatine are male sterile, insensitive to methyl jasmonate, and resistant to a bacterial pathogen. Plant Cell 6:751–759

Fischer D, Eisenberg D (1996) Fold recognition using sequence-derived predictions. Protein Sci 5:947–955

Forsthoefel NR, Wu Y, Schulz B, Bennett MJ, Feldmann KA (1992) T-DNA insertion mutagenesis in *Arabidopsis*: prospects and perspectives. Aust J Plant Physiol 19:353–366

Glover JA, Bloemer KC, Farrell LB, Chaudhury AM, Dennis ES (1996) Searching for tagged male-sterile mutants of *Arabidopsis*. Plant Mol Biol Rep 14:330–342

Glover J, Grelon M, Craig S, Chaudhury A, Dennis E (1998) Cloning and characterization of *MS5* from *Arabidopsis*: a gene critical in male meiosis. Plant J 15:345–356

Goldberg RB, Beals TP, Sanders PM (1993) Anther development: basic principles and practical applications. Plant Cell 5: 1217–1229

Gottschalk W, Wolff G (1983) Monographs on theoretical and applied genetics 7: Induced mutations in plant breeding. Springer, Berlin Heidelberg New York

Gray J, Close PS, Briggs SP, Johal GS (1997) A novel suppressor of cell death in plants encoded by the *Lls1* gene of maize. Cell 89:25–31

Greenberg JT, Ausubel FM (1993) *Arabidopsis* mutants compromised for the control of cellular damage during pathogenesis and aging. Plant J 4:327–341

He C, Tirlapur U, Cresti M, Peja M, Crone DE, Mascarenhas JP (1996) An *Arabidopsis* mutant showing aberrations in male meiosis. Sex Plant Reprod 9:54–57

Hebsgaard SM, Korning PG, Tolstrup N, Engelbrecht J, Rouze P, Brunak S (1996) Splice site prediction in *Arabidopsis thaliana* pre-mRNA by combining local and global sequence information. Nucl Acids Res 24:3439–3452

Hernandez Torres J, Chatellard P, Stutz E (1995) Isolation and characterization of *gmsti*, a stress-inducible gene from soybean (*Glycine max*) coding for a protein belonging to the TPR (*tetratrico*peptide repeats) family. Plant Mol Biol 27:1221–1226

Hulskamp M, Kopczak SD, Horejsi TF, Kihl BK, Pruitt RE (1995) Identification of genes required for pollen-stigma recognition in *Arabidopsis thaliana*. Plant J 8:703–714

Hulskamp M, Parekh NS, Grini P, Schneitz K, Zimmermann I, Lolle SJ, Pruitt RE (1997) The *STUD* gene is required for male-specific cytokinesis after telophase II of meiosis in *Arabidopsis thaliana*. Dev Biol 187:114–124

Jimenez G, Yacel J, Rowley R, Subramani S (1992) The *rad3*+ gene of *Schizosaccharomyces pombe* is involved in multiple check point functions and in DNA repair. Proc Natl Acad Sci USA 89:4952–4956

Jofuku KD, Goldberg RB (1988) Analysis of plant gene structure. In: Shaw CH (ed) Plant molecular biology: a practical approach. IRL Press, Oxford, pp 37–66

Kamalay JC, Goldberg RB (1980) Regulation of structural gene expression in tobacco. Cell 19:935–946

Kamalay JC, Goldberg RB (1984) Organ-specific nuclear RNAs in tobacco. Proc Natl Acad Sci USA 81:2801–2805

Kaneko T, Kotanii H, Nakamura Y, Sato S, Asamizu E, Miyajima N, Tabata S (1998) Structural analysis of *Arabidopsis thaliana* chromosome 5. V. Sequence features of the regions of 1,381,565 bp covered by 21 physically assigned P1 and TAC clones. DNA Res 5:131–145

Kaul MLH (1988) Male sterility in higher plants. Springer, Berlin Heidelberg New York

Keijzer CJ (1987) The process of anther dehiscence and pollen dispersal: 1. The opening mechanism of longitudinally dehiscing anthers. New Phytol 105:487–498

Klucher KM, Chow H, Reiser L, Fischer RL (1996) The *AINTEGUMENTA* gene of *Arabidopsis* required for ovule and female gametophyte development is related to the floral homeotic gene *APETALA2*. Plant Cell 8:137–153

Kneller G, Cohen FE, Langridge R (1990) Improvements in protein secondary structure prediction by an enhanced neural network. J Mol Biol 214:171–182

Koltunow AM, Truettner J, Cox KH, Wallroth M, Goldberg RB (1990) Different temporal and spatial gene expression patterns occur during anther development. Plant Cell 2:1201–1224

Komaki MK, Komaki M, Nishino E, Shimura Y (1988) Isolation and characterization of novel mutants of *Arabidopsis thaliana* defective in flower development. Development 104:195–204

Mariani C, Debeuckeleer M, Truettner J, Leemans J, Goldberg RB (1990) Induction of male-sterility in plants by a chimaeric ribonuclease gene. Nature 347:737–741

Marks MD, West J, Weeks DP (1987) The relatively large beta-tubulin gene family of *Arabidopsis* contains a member with an unusual transcribed 5′ noncoding sequence. Plant Mol Biol 10:91–104

Mauseth JD (1988) Plant anatomy. Benjamin/Cunnings, Menlo Park, N.J.

McConn M, Browse J (1996) The critical requirement for linolenic acid is pollen development, not photosynthesis, in an *Arabidopsis* mutant. Plant Cell 8:403–416

McNevin JP, Woodward W, Hannoufa A, Feldmann KA, Lemieux B (1993) Isolation and characterization of *eceriferum* (*CER*) mutants induced by T-DNA insertions in *Arabidopsis thaliana*. Genome 36:610–618

Modrusan Z, Reiser L, Feldmann KA, Fischer RL, Haughn GW (1994) Homeotic transformation of ovules into carpel-like structures in *Arabidopsis*. Plant Cell 6:333–349

Moffatt B, Somerville C (1988) Positive selection for male-sterile mutants of *Arabidopsis* lacking adenine phosphoribosyl transferase activity. Plant Physiol 86:1150–1154

Murray MG, Thompson WF (1980) Rapid isolation of high-molecular-weight plant DNA. Nucl Acids Res 8:4321–4325

Nakai K, Kanehisa M (1992) A knowledge base for predicting protein localization sites in eukaryotic cells. Genomics 14: 897–911

Okada K, Shimura Y (1994) Genetic analyses of signalling in flower development using *Arabidopsis*. Plant Mol Biol 26: 1357–1377

Peirson BN, Owen HA, Feldmann KA, Makaroff CA (1996) Characterization of three male-sterile mutants of *Arabidopsis thaliana* exhibiting alterations in meiosis. Sex Plant Reprod 9:1–16

Peirson BN, Bowling SE, Makaroff CA (1997) A defect in synapsis causes male sterility in a T-DNA-tagged *Arabidopsis thaliana* mutant. Plant J 11:659–669

Preuss D, Lemieux B, Yen G, Davis RW (1993) A conditional sterile mutation eliminates surface components from *Arabidopsis* pollen and disrupts cell signaling during fertilization. Genes Dev 7:974–985

Preuss D, Rhee SY, Davis RW (1994) Tetrad analysis possible in *Arabidopsis* with mutation of the *QUARTET* (*QRT*) genes. Science 264:1458–1460

Redei GP, Koncz C (1992) Classical mutagenesis. In: Koncz C, Chua N-H, Schell J (eds) Methods in *Arabidopsis* research. World Scientific, Singapore, pp 16–82

Regan SM, Moffatt BA (1990) Cytochemical analysis of pollen development in wild-type *Arabidopsis* and a male-sterile mutant. Plant Cell 2:877–889

Reiser L, Modrusan Z, Margossian L, Samach A, Ohad N, Haughn GW, Fischer RL (1995) The *BEL1* gene encodes a homeodomain protein involved in pattern formation in the *Arabidopsis* ovule primordium. Cell 83:735–742

Rick CM (1948) Genetics and development of nine male-sterile tomato mutants. Hilgardia 18:599–633

Ross KJ, Fransz P, Armstrong SJ, Vizir I, Mulligan B, Franklin FCH, Jones GH (1997) Cytological characterization of four meiotic mutants of *Arabidopsis* isolated from T-DNA-transformed lines. Chromosome Res 5:551–559

Sari-Gorla M, Ferrario S, Villa M, Pè ME (1996) *gaMS-1*, a gametophytic male-sterile mutant in maize. Sex Plant Reprod 9:216–220

Sari-Gorla M, Gatti E, Villa M, Pè ME (1997) A multi-nucleate male-sterile mutant of maize with gametophytic expression. Sex Plant Reprod 10:22–26

Sessions RA, Zambryski PC (1995) *Arabidopsis* gynoecium structure in the wild type and in *ettin* mutants. Development 121:1519–1532

Sessions A, Nemhauser JL, McColl A, Roe JL, Feldmann KA, Zambryski PC (1997) *ETTIN* patterns the *Arabidopsis* floral meristem and reproductive organs. Development 124:4481–4491

Sikorski RS, Boguski MS, Goebl M, Hieter P (1990) A repeating amino acid motif in *CDC23* defines a family of proteins and a new relationship among genes required for mitosis and RNA synthesis. Cell 60:307–317

Smyth DR, Bowman JL, Meyerowitz EM (1990) Early flower development in *Arabidopsis*. Plant Cell 2:755–767

Snustad DP, Haas NA, Kopczak SD, Silflow CD (1992) The small genome of *Arabidopsis* contains at least nine expressed *β-tubulin* genes. Plant Cell 4:549–556

Spurr AH (1969) A low viscosity epoxy resin embedding medium for electron microscopy. J Ultrastruct Res 26:31–43

Staiger CJ, Cande WZ (1990) Microtubule distribution in *dv*, a maize meiotic mutant defective in the prophase to metaphase transition. Dev Biol 138:231–242

Staiger CJ, Cande WZ (1993) Cytoskeletal analysis of maize meiotic mutants. In: Ormrod JC, Francis D (eds) Molecular and cell biology of the plant cell cycle. Kluwer, Dordrecht, pp 157–171

Taylor PE, Glover JA, Lavithis M, Craig S, Singh MB, Knox RB, Dennis ES, Chaudhury AM (1998) Genetic control of male fertility in *Arabidopsis thaliana*: structural analyses of postmeiotic developmental mutants. Planta 205:492–505

Van Der Veen JH, Wirtz P (1968) EMS-induced genic male-sterility in *Arabidopsis thaliana*: a model selection experiment. Euphytica 17:371–377

Yadegari R, de Paiva GR, Laux T, Koltunow AM, Apuya N, Zimmerman JL, Fischer RL, Harada JJ, Goldberg RB (1994) Cell differentiation and morphogenesis are uncoupled in *Arabidopsis raspberry* embryos. Plant Cell 6:1713–1729

Zambryski P, Holsters M, Kruger K, Depicker A, Schell J, Montagu MV, Goodman HM (1980) Tumor DNA structure in plant cells transformed by *A. tumefaciens*. Science 209:1385–1391